SKBF KBS TEKNISK RAPPORT

82-01

# Hydrothermal conditions around a radioactive waste repository Part 3 – Numerical solutions for anisotropy

Roger Thunvik
Royal Institute of Technology, Stockholm, Sweden

Carol Braester
Institute of Technology, Haifa, Israel

December 1981

SVENSK KÄRNBRÄNSLEFÖRSÖRJNING AB / AVDELNING KBS

*POSTADRESS: Box 5864, 102 48 Stockholm, Telefon 08-67 95 40*

# HYDROTHERMAL CONDITIONS AROUND A RADIOACTIVE WASTE REPOSITORY

## Part 3 - Numerical Solutions for Anisotropy

Roger Thunvik
Royal Institute of Technology, Stockholm, Sweden

Carol Braester
Israel Institute of Technology, Haifa, Israel

December 1981



A list of other reports published in this series during 1982, is attached at the end of this report. Information on KBS technical reports from 1977-1978 (TR 121), 1979 (TR 79-28), 1980 (TR 80-26) and 1981 (TR 81-17) is available through SKBF/KBS.

# HYDROTHERMAL CONDITIONS AROUND A RADIOACTIVE WASTE REPOSITORY

## Part 3 - Numerical Solutions for Anisotropy

Roger Thunvik
Royal Institute of Technology
Stockholm, Sweden

Carol Braester
Israel Institute of Technology
Haifa, Israel

December 1981

## ABSTRACT

Numerical solutions for the hydrothermal conditions around a hard rock repository for nuclear fuel waste are presented. The objective of the present investigation is to illustrate in principle the effect of heat released from a hypothetical radioactive waste repository with regard to anisotropy in the rock permeability. Permeability and porosity are assumed to be constant or to decrease exponentially with depth. The hypothetical repository is situated below a horizontal ground surface or below the crest of a hill, and it is assumed that the water table follows the topography. Major interest in the analysis is directed towards the influence of anisotropy in the permeability on the flow patterns and travel times for water particles, being traced from the repository to the ground surface. The presented results show that anisotropy in the permeability may have a significant influence on the flow conditions around the repository and subsequently also on the travel times from the repository.

# CONTENTS

## SUMMARY AND CONCLUSIONS

This report presents a number of numerical solutions for the flow of groundwater and heat through anisotropic rock around a hypothetical radioactive waste repository. The presented cases illustrate the hydrothermal conditions around a radioactive waste repository which is situated below (i) a horizontal ground surface, or (ii) the crest of a hill. Each of the two cases is analyzed with regard to constant as well as decreasing permeability with depth. The present investigation should be seen as an extension of a previous one, in which the permeability of the rock around the repository was assumed to be isotropic.

Generally, the results of the calculations show that anisotropy in the rock permeability, especially in the vertical direction, may be an important factor for the groundwater flow around a radioactive waste repository. The most significant effect due to anisotropy in the rock formation is observed in the examples, in which permeability and porosity are assumed to be constant over the considered flow domain. Conversely, the effect of anisotropy is less significant in the examples where the rock permeability is assumed to decrease with depth. In consequence of the results obtained from the present investigation, it is suggested that anisotropy in the rock permeability be determined in connection with the permeability tests, which have to be carried out in situ for a prospective radioactive waste repository.

The numerical solutions for a repository situated below a horizontal ground surface and constant permeability, resulted in a very short travel time, about 400 years for vertical anisotropy, and

about 4400 years for horizontal anisotropy. If decreasing permeability with depth is assumed, then none of the water particles starting from the repository will reach the ground surface for either vertical or horizontal anisotropy. This suggests, that in this setting the effect of decreasing permeability with depth on the flow conditions is greater than that of anisotropy.

For a repository situated below the crest of a hill, the shortest travel time is obtained for vertical anisotropy and constant permeability over the flow domain. Then, the shortest travel time is calculated to be about 1000 years. The corresponding travel times for isotropy and horizontal anisotropy are about four times longer. If decreasing permeability with depth is assumed, then the travel time is about 4000 years for both isotropy and horizontal anisotropy, and about 6000 years for vertical anisotropy. Thus, when assuming decreasing permeability with depth, then the travel time for isotropy is shorter than for vertical as well as for horizontal anisotropy in the rock permeability. This applies also for steady flow, while neglecting the effect of the heat from the repository.

## General assumptions

The objective of the present investigation is to illustrate in principle the significance of anisotropy in the permeability to the groundwater flow patterns. Therefore, simplified assumptions are made regarding the properties of the flow domain as well as the repository to facilitate the interpretation of the results of the calculations.

The flow domain is bounded downwards by an impervious bottom, laterally by noflow boundaries and upwards by the water table, which is assumed to coincide with the ground surface is considered. Permeability is assumed to be constant or to decrease exponentially with depth over the flow domain, and the principal directions of the anisotropy are assumed to coincide with the horizontal respectively vertical directions of the considered flow domain. The initial flow pattern is assumed to be governed by the topography and the natural geothermal gradient, which here is assumed to be 30 degrees Celsius/km.

A radioactive waste repository located at a depth of about 500 metres below the ground surface is considered. The lateral extent of the repository is about 1 km. The repository consists of a system of parallel tunnels, spaced 25 metres apart, and the radioactive waste is stored in canisters in drillholes along the bottoms of the tunnels. Thus, a repository with a lateral extent of 1 km contains 41 tunnels. The drillholes for disposal of the canisters are spaced out every 4 metres, along the bottom of each tunnel. The thermal load per canister, at the moment of disposal, is assumed to be 525 W, resulting in a uniformly distributed load of 5.25 W/sq.m over the area of the repository. For simplicity in the calculations the waste is assumed to be instantaneously emplaced.

The numerical examples are organized into two main cases with regard to the topography above the repository. Four examples are worked out for each of the two cases. These are:

1. Constant permeability and porosity over the flow domain and vertical anisotropy.

2. Constant permeability and porosity over the flow domain and horizontal anisotropy.
3. Exponentially decreasing permeability and porosity with depth over the flow domain and vertical anisotropy.
4. Exponentially decreasing permeability and porosity with depth over the flow domain and horizontal anisotropy.

In the examples with vertical anisotropy, the permeability in the vertical direction is 10 times higher than the permeability in the horizontal direction, and in the examples with horizontal anisotropy the horizontal permeability is 10 times higher than the permeability in the vertical direction. The values of the permeability components are chosen such that (i) the isotropic equivalent permeability is the same for vertical as well as horizontal anisotropy, and (ii) the examples in the present investigation may be compared with those in a previous one, in which the rock permeability generally was assumed to be isotropic.

The results are presented in the form of tables of flow times for water particles to travel from the repository to the ground surface and in the form of pathlines. The hydrothermal flow conditions are illustrated by vector plots showing the direction and magnitude of the groundwater fluxes, and isotherms showing the temperature distribution at different moments. Below follows a brief presentation of the results obtained from the calculations.

<u>Repository situated below a horizontal ground surface</u>

In this case, the shortest travel time for a water particle is obtained in <u>example 1</u>, in which vertical anisotropy and constant permeability are assumed over the flow domain. The travel time for each of the water particles starting within a distance of about 300 metres from the centre of the repository is computed to be about 400 years. Two of the traced water particles do not reach the ground surface at all. One of these two water particles is traced from a point at a distance of 100 metres from the edge of the repository and the other is traced from the edge of the repository.

In example 2, horizontal anisotropy in the permeability is assumed. The shortest travel time is computed to be about 4400 years. In fact, only the water particle starting from the centre of the repository will reach the ground surface. Thus, the water particle starting from the centre of the repository moves straight up to the ground surface, while the other water particles are getting involved in the convection cell, being formed around the edge of the repository. As time proceeds, the groundwater flow abates due to the radioactive decay, and as a result none of the other water particles will reach the ground surface.

The two travel times, obtained from examples 1 and 2, may be compared with the corresponding travel time for isotropic conditions. In a previous investigation this was calculated to be about 650 years.

In examples 3 and 4, none of the water particles traced from the repository will reach the ground surface. This is due to the fact that the groundwater movements are so slow in the region around the repository, and that the radioactive heat source will decay, before any water particles will reach the ground surface. The comparatively slow groundwater movements are due to the decrease in permeability with depth, that is assumed in these two examples.

Repository situated below the crest of a hill

The repository is assumed to be symmetrically situated below the crest of a hill with a slope of one per mille of each hillside. This means, that the groundwater flow will be governed by the heat released from the repository as well as the topographical gradient.

Also in this case the shortest break-through time is obtained in example 1, in which constant permeability and vertical anisotropy are assumed. The shortest travel time from the repository to the ground surface is obtained for a water particle starting at a distance of about 100 metres from the repository, and the travel time for this water particle is calculated to be about 1000 years. For steady flow the shortest travel time is calculated to be about 3000 years. The corresponding figures for the isotropic equivalent permeability were previously calculated to be about 4000 years and 2500 years, respectively. This means, that the effect of vertical anisotropy on the travel times is greatest, when the heat released from the repository is taken into account.

The horizontal anisotropy assumed in example 2, resulted in considerably longer travel times in comparison with those obtained for vertical anisotropy as well as isotropy in the rock permeability. The shortest travel time for steady state conditions is about 9000 years, which is about 3 times longer than for vertical anisotropy and about 3.5 times longer than for isotropy. When the heat from the repository is taken into account the travel times become extremely long. Then, the travel times are calculated to be over 60000 years for all water particles but one, namely the water particle being traced from the centre of the repository, and the travel time for this water particle is calculated to be about 4100 years.

In examples 3 and 4, permeability and porosity are assumed to decrease exponentially with depth over the flow domain. The shortest travel times are obtained for steady flow conditions. In the example with vertical anisotropy the steady state travel time is about 4500 years, and in the example with horizontal anisotropy it is about 3200 years. For isotropic permeability the corresponding travel time was previously computed to be about 2000 years. When taking the heat released from the repository into account, the shortest travel time is about 5800 years for vertical anisotropy, about 4100 years for horizontal anisotropy, and about 3900 years for isotropic permeability.

## NOMENCLATURE

| Symbol | Description | Dimension | SI unit |
|---|---|---|---|
| $c$ | compressibility | $M^{-1}LT^{2}$ | 1/Pa |
| $C$ | specific heat capacity | $L^{2}T^{-2}K^{-1}$ | J/(kgK) |
| $g$ | acceleration of gravity | $LT^{-2}$ | $m/s^2$ |
| $k_r$ | multiplier to relate the flow rate in an anisotropic medium to that of an isotropic equivalent one | - | - |
| $k_{r\underline{ii}}$ | multiplier to relate the permeability in the i-direction to the isotropic equivalent permeability | - | - |
| $k$ | permeability | $L^2$ | $m^2$ |
| $p$ | pressure | $ML^{-1}T^{-2}$ | Pa |
| $q$ | specific discharge | $LT^{-1}$ | m/s |
| $Q$ | flow rate | $M^{3}T^{-1}$ | $m^3/s$ |
| $t$ | time | T | s |
| $T$ | temperature | K | K |
| $x_i$ | Cartesian coordinate | L | m |
| $X_i$ | Cartesian coordinate in an isotropic equivalent medium | L | m |
| $\beta$ | coefficient of thermal volume expansion of the fluid | $K^{-1}$ | 1/K |
| $\Delta$ | difference | - | - |
| $\lambda$ | thermal conductivity | $MLT^{-3}K^{-1}$ | W/(mK) |
| $\mu$ | dynamic viscosity | $ML^{-1}T^{-1}$ | Pas |
| $\rho$ | density | $ML^{-3}$ | $kg/m^3$ |
| $\phi$ | porosity | - | - |
| $\tau$ | time transformed from an anisotropic medium into an isotropic equivalent one | T | s |

superscripts

| | |
|---|---|
| f | fluid |
| r | rock |
| * | equivalent medium |
| o | reference value |

subscripts

| | |
|---|---|
| i,j | indices used for Cartesian tensor notation, repeated indices indicate summation over these indices (i=j=1,2,3) |

| | |
|---|---|
| $p_{,t}$ | partial time derivative of p |
| $p_{,j}$ | gradient of p |

Note: underlined indices indicate that no summation is
is to be performed over these indices

# 1. INTRODUCTION

The objective of the present investigation is to exemplify in principle the effect of anisotropy in the rock permeability around a radioactive waste repository on the groundwater flow pattern under various conditions. This report deals with a number of numerical examples worked out in order to illustrate the influence of a hypothetical radioactive waste repository on the groundwater flow around the repository. Thus, no specific site is referred to in the analysis and the assumptions regarding the characteristics of the flow domain as well as the repository are made simple to facilitate the interpretation of the results.

The mathematical flow model used in the calculations is thoroughly described in a previous report entitled "HYDROTHERMAL CONDITIONS AROUND A RADIOACTIVE WASTE REPOSITORY, Part 1 - A Mathematical Model for the Flow of Groundwater and Heat in Fractured Rock". For this reason the governing equations used in the present study will be given without derivation in this report.

The present study should be seen as an extension of a previous investigation, in which the effect of the heat released from a repository in the groundwater flow patterns was studied. However, in the previous investigation the rock permeability was assumed to be isotropic in all of the numerical examples. The examples with isotropic permeability are presented in part 2 of the above mentioned report. With the exception of rock permeability, the assumptions regarding the input data and boundary conditions are the same in the present investigation as in the previous one. In order to facilitate a comparison between the two investigations the values of the anisotropic permeability components are chosen such that, when transforming the anisotropic media considered into isotropic equivalent ones, the permeability becomes the same as in the previous investigation.

It should be mentioned, however, that there is little information available at present regarding anisotropy in the rock permeability. This means, that the importance of the obtained results is highly dependent on the relevance of the assumed anisotropy in the rock formation. The field measurements currently being carried out are largely based on one hole measurements. In these tests the rock permeability is determined at certain intervals, being sealed off by double packers, along the borehole. A serious shortcoming is that the values of the permeability obtained from these tests represent the horizontal permeability component only, and that no information is obtained about the permeability in the vertical direction. As a matter of fact, the method used for the interpretation of these permeability tests presupposes that the rock formation under consideration is isotropic as well as homogeneous.

The remaining part of this report is organized as follows: Chapter 2 deals with the flow model. In the first section of this chapter the governing equations are presented. The second section is devoted to the relation between an anisotropic medium and an isotropic equivalent one. The third section is devoted to a simple qualitative analysis, using the transformations derived in the second section of chapter 2. Chapter 3 deals with the input data and boundary conditions. Chapter 4 contains the presentation and discussion about the numerical examples worked out.

# 2. THE FLOW MODEL

The mathematical flow model used herein consists of a set of partial differential equations describing the flow of mass and heat through a fractured rock formation. The model equations are solved numerically using the finite element method. The model is based on the continuum approach, implying that various properties such as permeability, pressure, fluid and rock temperature are defined as averages over some volume elements. These elements must be large in comparison with individual fractures, but small with regard to the dimensions of the exterior boundaries of the rock formation under consideration.

The model may treat the fractured rock either as a single equivalent continumm representing both fluid and rock, or as two overlapping continua, where one represents the fluid in the fractures and the other the solid rock. It was concluded that the heat flow under the present conditions is dominated by conduction. Then the fracture pattern and the solid blocks may be treated as a single equivalent medium. This approach assumes that local thermal equilibrium between the fluid and the rock is reached instantaneously.

## 2.1 Governing equations of the flow model

The following set of governing equations is used for the present study:

(i) an equation for the fluid flow

$$\phi\rho^f(c^f + c^r)\,p_{,t} - \phi\rho^f \beta T_{,t} - (\rho^f \frac{k}{\mu}_{ij}\,(p_{,j} - \rho^f g_j))_{,i} = 0 \tag{2.1}$$

where $\phi$ is porosity, $\rho^f$ is fluid density, cf is fluid compressibility, $c^r$ is rock compressibility, p is pressure, $\beta$ is the thermal volume expansion coefficient, T is temperature, $k_{ij}$ is the permeability tensor, $\mu$ is dynamic viscosity and g is the acceleration of gravity, and

(ii) an equation for the heat flow

$$-\ (\rho C)^* \, T_{,t} - (\lambda^* T_{,i})_{,i} + \rho^f C^f q_i T_{,i} = 0 \tag{2.2}$$

where $\lambda^*$ denotes the thermal conductivity and $(\rho C)^*$ the volumetric heat capacity of the single equivalent medium representing both the fluid and rock media, $C^f$ is the heat capacity of the fluid and q is the Darcy velocity. Darcy's law is expressed by

$$q_i = -\frac{k}{\mu}_{ij}\,(p_{,j} - \rho^f g_j) \tag{2.3}$$

In addition to the previous equations, there are two equations of state relating the density and viscosity of the fluid to pressure and temperature

$$\rho^f = \rho(p,T) \tag{2.4}$$

$$\mu = \mu(T) \tag{2.5}$$

The previous set of governing equations is solved numerically using a finite element Galerkin method. A discussion of the flow model developed is given in a previous report entitled "HYDROTHERMAL CONDITIONS AROUND A RADIOACTIVE WASTE REPOSITORY (KBS: 80-19).

## 2.2 Equations for an isotropic equivalent medium

In this section a set of transformations is defined in order to transform an anisotropic medium into an isotropic equivalent one, vice versa. In the present analysis a two-dimensional vertical flow domain with anisotropy in the permeability is considered. The principal directions of the anisotropy are assumed to coincide with the coordinate axes. Thus, the permeability tensor reduces to its diagonal.

It is assumed that the permeability tensor at a given point may be obtained by multiplying an isotropic permeability tensor by a certain coefficient $k_{rij}$ in the following way:

$$k_{ii}(x_i) = k_{r\underline{ii}}k(x_i) \tag{2.6}$$

Dividing equations (2.1) and (2.2) by kr22, we obtain

$$\frac{1}{k_{r22}} \phi\rho^f (c^f + c^r)\, p_{,t} - \frac{1}{k_{r22}} \phi\rho^f \beta T_{,t}$$

$$- \left(\frac{k_{r\underline{i}\underline{i}}}{k_{r22}}\right) \left(\rho^f \frac{k}{\mu} (p_{,i} - \rho^f g_i)\right)_{,i} = 0 \tag{2.7}$$

for the fluid flow equation, and

$$\frac{1}{k_{r22}} (\rho C)^* \, T_{,t} - \frac{1}{k_{r22}} (\lambda^* T_{,i})_{,i}$$

$$- \rho^f C^f \left(\frac{k_{r\underline{i}\underline{i}}}{k_{r22}}\right) \rho^f \frac{k}{\mu} (p_{,i} - \rho^f g_{,i})\, T_{,i} = 0 \tag{2.8}$$

for the heat flow equation.

The term $(k_{r\underline{i}\underline{i}}/k_{r22})$ is enclosed in parentheses to indicate that the equations are written in symbolic form. This means, that they cannot be reduced by $k_{r22}$ Note also that no summation is to be performed over the underlined indices.

The following geometrical transformations of the flow domain are made to obtain an isotropic equivalent medium with regard to permeability.

$$X_1 = (k_{r22}/k_{r11})^{\frac{1}{2}}\, x_1 \tag{2.9}$$

and

$$X_2 = x_2 \tag{2.10}$$

Substitution of (2.9) and (2.10) into (2.7) and (2.8) gives

$$\frac{1}{k_{r22}} \phi\rho^f (c^f + c^r)\, p_{,t} - \frac{1}{k_{r22}} \phi\rho^f \beta T_{,t}$$

$$- (\rho^f \frac{k}{\mu} (p_{,i} - \rho^f g_i))_{,i} = 0 \tag{2.11}$$

and

$$\frac{1}{k_{r22}} (\rho C)^* \, T_{,t} - \frac{1}{k_{r22}} (\lambda^* T_{,i})_{,i}$$

$$- \rho^f C^f (\rho^f \frac{k}{\mu} (p_{,i} - \rho^f g_i))\, T_{,i} = 0 \tag{2.12}$$

The flow rate in the $x_2$-direction, using Darcy's law, is expressed by

$$Q_2 = \quad q_2 \, \Delta x_1 \tag{2.13}$$

or

$$Q_2 = - k_{r22} \frac{k}{\mu} (p_{,2} - \rho^f g_2)\, \Delta x_1 \tag{2.14}$$

Applying the transformations given by (2.9) and (2.10), we obtain the flow rate for the isotropic equivalent medium, by using the following expression for the permeability multiplier

$$k_r = (k_{r11}/k_{r22})^{\frac{1}{2}} \tag{2.15}$$

Multiplying equations (2.11) and (2.12) by $k_r$, we obtain

$$\left(\frac{k_{r11}}{k_{r22}}\right)^{\frac{1}{2}} \phi\rho(c^f + c^r)\, p_{,t} - \left(\frac{k_{r11}}{k_{r22}}\right)^{\frac{1}{2}} \phi\rho^f \beta\, T_{,t}$$

$$- k_r(\rho^f \frac{k}{\mu}\,(p_{,i} - \rho^f g_i))_{,i} = 0 \qquad (2.16)$$

for the fluid flow equation, and

$$\left(\frac{k_{r11}}{k_{r22}}\right)^{\frac{1}{2}} (\rho C)^*\, T_{,t} - \left(\frac{k_{r22}}{k_{r11}}\right)^{\frac{1}{2}} (\lambda^* T_{,1})_{,1} - \left(\frac{k_{r11}}{k_{r22}}\right)^{\frac{1}{2}} (\lambda^* T_{,2})_{,2}$$

$$- k_r(\rho^f \frac{k}{\mu}\,(p_{,i} - \rho^f g_i))\, T_{,i} = 0 \qquad (2.17)$$

for the heat flow equation.

Equations (2.16) and (2.17) suggest the following transformation of the time scale, when transforming the anisotropic permeability into an isotropic equivalent permeability

$$\tau = (k_{r22}/k_{r11})^{\frac{1}{2}}\, t \qquad (2.18)$$

Substituting the previous relation into (2.16) and (2.17), we obtain

$$\phi\rho^f (c^f + c^r)\, p_{,\tau} - \phi\rho^f \beta T_{,\tau}$$

$$- k_r(\rho^f \frac{k}{\mu}\,(p_{,i} - \rho^f g_i)_{,i} = 0 \qquad (2.19)$$

for the fluid flow equation, and

$$(\rho C)^* \, T_{,\tau} - \left(\frac{k_{r22}}{k_{r11}}\right)^{\frac{1}{2}} (\lambda^* T_{,1})_{,1} - \left(\frac{k_{r11}}{k_{r22}}\right)^{\frac{1}{2}} (\lambda^* T_{,2})_{,2}$$

$$- k_r (\rho^f \frac{k}{\mu} (p_{,i} - \rho^f g_i)) \, T_{,i} = 0 \qquad (2.20)$$

for the heat flow equation.

Equation (2.19) is the fluid flow equation for the isotropic equivalent medium, and equation (2.20) is the heat flow equation, when using the suggested transformations. Note that when applying these transformations to the equation for the heat flow, the originally isotropic thermal conductivity becomes anisotropic according to the following relationships

$$\lambda_{11} = (k_{r22}/k_{r11})^{\frac{1}{2}} \, \lambda^* \qquad (2.21)$$

and

$$\lambda_{22} = (k_{r11}/k_{r22})^{\frac{1}{2}} \, \lambda^* \qquad (2.22)$$

This means, that when transforming an anisotropic medium into an isotropic equivalent one, not only the geometrical characteristics of the flow domain are changed, but also the time scale and material properties. Therefore, care should be taken in drawing conclusions, regarding the flow through an anisotropic medium, based on solutions for an isotropic medium.

## 2.3 Qualitative analysis

This section contains a simple analysis of the relation between an anisotropic medium and an isotropic one, making use of the transformations derived in the previous section. In the numerical examples being presented in the sequel, the initial temperature distribution is assumed to follow the geothermal gradient. Furthermore, a single level repository with a horizontal extent that is many times larger than the vertical one is assumed. Thus, the thermal gradient is essentially vertical in the flow region studied, except for in the region close to the lateral edges of the repository. Therefore, the present qualitative analyis can be simplified by neglecting the horizontal thermal gradients. This means, that the equivalent thermal conductivity in the $x_1$-direction obtained by the previous transformation will have little influence on the flow problem, and that equations (2.19) and (2.20) may be assumed to represent an isotropic equivalent medium also with regard to the heat flow.

Let us consider a solution to an isotropic flow problem in the $X_i$ (i=1,2) - plane. The anisotropic equivalent solution depends on the ratio of the previously defined permeability multipliers according to the following relationships

$$x_1 = (k_{r11}/k_{r22})^{\frac{1}{2}} \qquad (2.23)$$

$$x_2 = X_2 \qquad (2.24)$$

$$t = (k_{r11}/k_{r22})^{\frac{1}{2}} \tau \qquad (2.25)$$

$$\lambda^* = (k_{r22}/k_{r11})^{\frac{1}{2}}\lambda_{22} \qquad (2.26)$$

Thus, when using a solution for an isotropic medium to study an anisotropic medium with horizontal anisotropy ($k_{r11} > k_{r22}$), the solution for the anisotropic medium is obtained by constricting the isotropic medium in the $x_1$-direction according to the relationship given above (2.22). Furthermore, the characteristic time is reduced and the thermal conductivity is increased using the relationships (2.24) and (2.25). This means, that a circular flow pattern will be transformed into an elliptic one with the principle axis in the $x_2$-direction. As a result, the travel times for water particles flowing from the repository to the ground surface will be affected.

Thus, for an idealized flow problem in which the repository is assumed to be located below a horizontal water table, the travel times become longer when transforming the equivalent isotropic flow domain into an anisotropic one. If instead the anisotropy is vertical ($k_{r11} < k_{r22}$), then the effect on the travel times will be the opposite, i.e. the travel times will become shorter in comparison with those obtained from the isotropic equivalent flow domain.

## 3. INPUT DATA

In this chapter there will be only a brief description of the input data used in the numerical examples worked out. A more thorough discussion about the input parameters and their relative significance has been presented in a previous report entitled: "HYDROTHERMAL CONDITIONS AROUND A RADIOACTIVE WASTE REPOSITORY, Part 2 - Numerical Solutions".

The dependence of the permeability upon the depth below the ground surface is assumed to be the same as in the above mentioned report, that is to say permeability is assumed to be constant or to decrease exponentially with depth over the flow domain. The same depth dependence as for the permeability is also assumed for porosity. In the presented examples flow patterns are studied for horizontal as well as vertical anisotropy. The anisotropy in the horizontal direction is assumed to be 10 times that of the vertical direction, vice versa.

The flow domain is represented by a two-dimensional vertical cross-section with a lateral extent of 3 km and a depth of 1.5 km. The hypothetical repository is located at a depth of about 500 metres below the ground surface. The lateral extent of the repository is 1 km, and the initial thermal load due to the repository is 5.25 $W/m^2$ . Two main cases are considered with regard to the topography or the position of the water table. The two cases are: (i) a repository situated in an area with a horizontal ground surface (figure 3.1), and (ii) a repository situated below the crest of a hill with linearly sloping sides (figure 3.2).

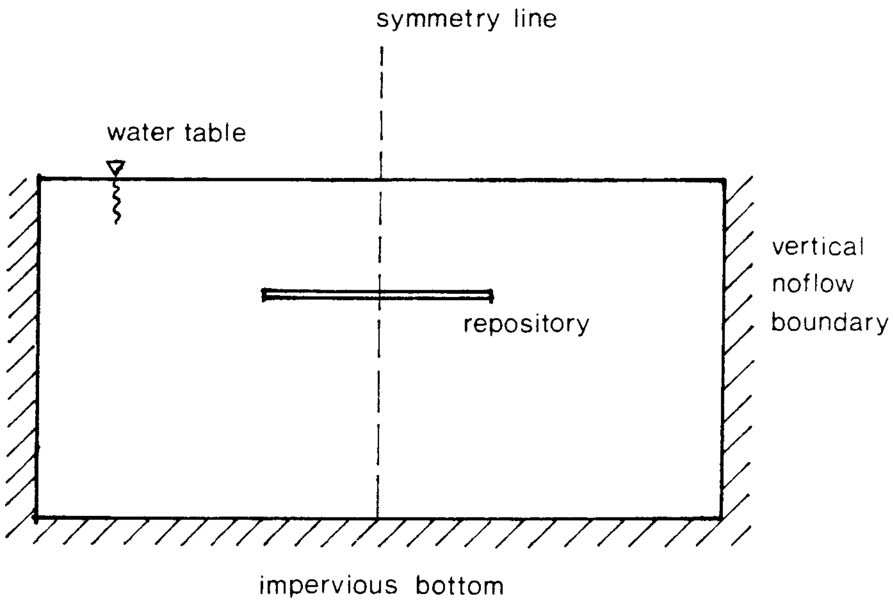


Figure 3.1 Case 1. A repository located in an area where the groundwater is horizontal.

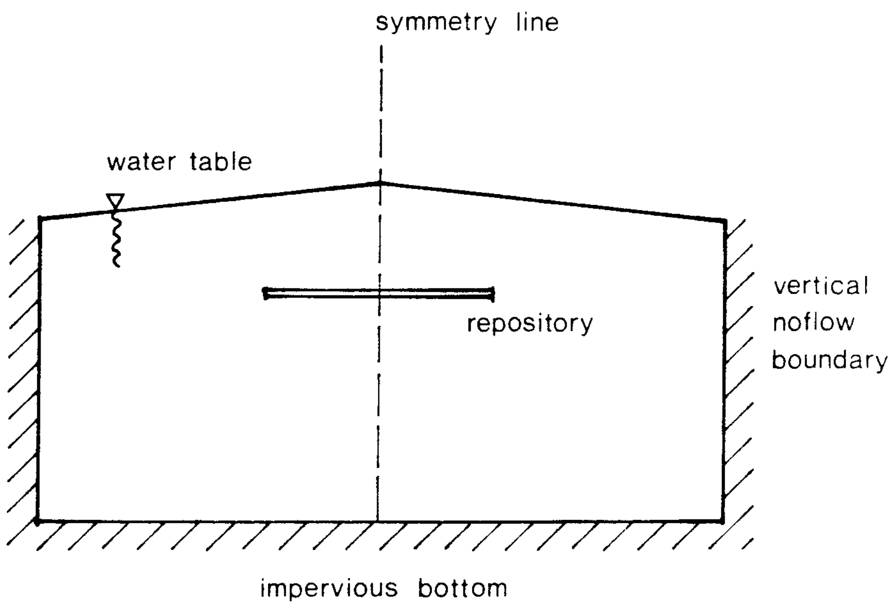


Figure 3.2 Case 2. A repository located below the crest of a hill.

The boundary conditions are: (i) constant pressure at the top boundary and (ii) no flow boundary conditions at the bottom and lateral boundaries, (iii) precribed temperature at the top and bottom boundaries, and (iv) adiabatic lateral boundaries.

The material properties assumed in the calculations are summarized in table 3.1 below.

Table 3.1 Summary of material properties used in the examples

| | | |
|---|---|---|
| Porosity at the ground surface | 0.003 | - |
| Permeability at the ground surface | 10-14 | $m^2$ |
| Fluid density | 998 | $kg/m^3$ |
| Dynamic viscosity | 0.001 | Pas |
| Fluid compressibility | 10-10 | 1/Pa |
| Thermal volume expansion of the fluid | 0.0018 | 1/K |
| Thermal conductivity of the fluid | 0.6 | W/(mK) |
| Specific heat capacity of the fluid | 4180 | J/(kgK) |
| Rock density | 2700 | $kg/m^3$ |
| Thermal conductivity of the rock | 3.5 | W/(mK) |
| Specific heat capacity of the rock | 800 | J/(kgK) |
| Rock compressibility | 10-11 | 1/Pa |
| Gravity | 9.81 | $m/s^2$ |

Fluid density and viscosity are given in the previous table as reference values corresponding to a temperature of 20 degrees Celsius. Using these values and a reference value of the isotropic equivalent permeability of 10-14 $m^2$, then the value of the hydraulic conductivity becomes about 10-7 m/s. The exponential decrease in the permeability with depth is in the examples

$$k = k^{o} e^{0.0092 z} \qquad (4.1)$$

Thus, at an elevation of -500 metres the value of isotropic equivalent permeability is 10-16 and at -1000 metres 10-18 $m^2$ and the corresponding values of the hydraulic conductivity are approximately 10-9 respectively 10-11 m/s.

The principal axes of the permeability tensor are assumed to be aligned with the horizontal respectively vertical directions of the flow domain. In the examples with vertical anisotropy the permeability in the vertical direction is assumed to be 10 times higher than the permeability in the horizontal direction, and in the examples with horizontal anisotropy the permeability in the horizontal direction is 10 times higher than the permeability in the vertical direction. The permeability values are chosen in such a way that the isotropic equivalent permeability becomes the same as the permeability assumed in the previous investigation, in which the rock permeability was assumed to be isotropic in all of the examples.

# 4. NUMERICAL SOLUTIONS

Two main cases are considered for the numerical solutions. Each case is defined by the geometry of the flow domain, boundary conditions and the location of the repository. The two cases are:

4.1 Repository located below a horizontal ground surface.

4.2 Repository located below the crest of a hill.

Each case is analysed for constant permeability and porosity respectively exponentially decreasing permeability and porosity with depth. The considered flow domain is symmetrical around the vertical centre line through the repository for both cases. Thus, only one half of the flow domain needs be analysed, reducing the computational work. The following results of the computations are presented for each case: exit times (travel times for water particles flowing from the repository to the ground surface), pathlines from the repository, groundwater fluxes and isotherms.

Flow times from the repository to the ground surface are calculated for water particles spaced out 100 metres apart along the repository. The results are presented in the form of tables of the flow times and graphical display of the pathlines. The calculations are performed for conditions with heat released from the repository as well as for undisturbed conditions, taking into account only the effects of topography and the natural geothermal gradient.

Groundwater fluxes are displayed graphically in the form of vector plots. The arrow of a vector indicates the flow direction and the length indicates the relative order of magnitude of the specific discharge. The velocities are logarithmically scaled in such a way that the maximum velocity at a certain instant corresponds to 1 centimetre on the graph. Isotherms are used to illustrate the temperature distribution over the flow domain. The difference in temperature between each isotherm is 5 degrees Celsius.

The element meshes used in the calculations were designed such that smaller elements were generated around the repository and larger elements towards the bottom and the lateral boundaries of the flow domain. In some of the examples, problems were encountered in the pathline trace due to the large elements towards the flow domain boundaries. The elements at the boundaries appeared to be too coarse to properly describe the sudden variation in the flow direction within these elements. As a consequence, some of the pathlines hit the boundaries. When this occurs, the pathline trace is continued along the boundary until, if possible, the ground surface is reached.

## 4.1 Repository located below a horizontal ground surface

This case illustrates a situation where the groundwater flow is induced only by heat released from the radioactive waste repository. In the initial stage, the groundwater is in hydrostatic equilibrium, assuming that the pressure gradient is vertical and parallel to the geothermal gradient over the entire flow domain.

Four examples are presented for this case. The four examples are organized as follows:

4.1.1 Repository located below horizontal ground surface. Constant permeability and porosity and vertical anisotropy in permeability.

4.1.2 Repository located below horizontal ground surface. Constant permeability and porosity and horizontal anisotropy in permeability.

4.1.3 Repository located below horizontal ground surface. Exponentially decreasing permeability and porosity with depth and vertical anisotropy in permeability.

4.1.4 Repository located below horizontal ground surface. Exponentially decreasing permeability and porosity with depth and horizontal anisotropy in permeability.

Generally, in these examples the groundwater flow pattern is characterized by upward movements at the repository and downward movements at the lateral boundary. Thus, outflow takes place through the part of the ground surface that lies above the repository and inflow through the remaining part. The assumption that the level of the water table is constant with time, implies that the outflowing water is removed from the ground surface by some process, and that there is sufficient recharge of surface water to the water table at the inflow area.

The exit time given in the beginning of each example corresponds to the travel time for the first water particle to reach the ground surface. Since the groundwater movements in these examples are caused only by the heat released from the repository, there are no travel times or pathlines to be considered when the groundwater is in equilibrium. Groundwater fluxes are displayed in the form of vectors and temperatures in the form of isotherms at the following times after the emplacement of the radioactive waste: 53, 360 and 1800 years.

4.1.1 Repository located below a horizontal ground surface. Permeability and porosity are constant over the flow domain. Vertical anisotropy.

Exit time: > 400 years

The results of the pathline trace are presented in table 4.1.1.

Pathlines are displayed in figure 4.1.1.

Groundwater fluxes and isotherms are displayed in figures 4.1.2 - 4.1.4.

Generally, the effect of the heat released from the repository is to cause an uplift of the groundwater at the repository. Therefore, the expected result of having vertical anisotropy is to obtain shorter travel times from the repository to the ground surface than for the isotropic equivalent flow conditions. This is also verified by the present example. The shortest travel times are obtained for water particles released near the centre of the repository. The travel time for the water particle traced from the very centre of the repository is about 400 years, while for isotropy in the permeability it was previously calculated to be about 650 years.

As can be seen in the figure with the graphical display of the pathlines, two of the pathlines do not reach the ground surface at all. Thus, the water particle traced from a point at a distance of 400 metres from the centre of the repository deviates from its original vertical course, following an elliptic path for some thousand years. Then the effect of the heat begin to vanish and as a result the groundwater movements stop. The water particle traced right from the edge of the repository is circulating closely around the edge in the initial stage. After approximately 1500 years this water particle continue to move upwards, until it stops at a depth of about 50 metres below the ground surface.

Table 4.1.1 Coordinates of the starting respectively end points and the corresponding travel times in years of path-lines traced from a radioactive waste repository situated below a horizontal ground surface. Permeability and porosity are constant over the flow domain. Vertical anisotropy.

| No | Starting point | | End point | | Travel time |
|---|---|---|---|---|---|
| 1 | 0 | -500 | 0 | 0 | 427 |
| 2 | 100 | -500 | 93 | 0 | 431 |
| 3 | 200 | -500 | 191 | 0 | 419 |
| 4 | 300 | -500 | 304 | 0 | 433 |
| 5 | 400 | -500 | - | - | No exit |
| 6 | 500 | -500 | - | - | No exit |

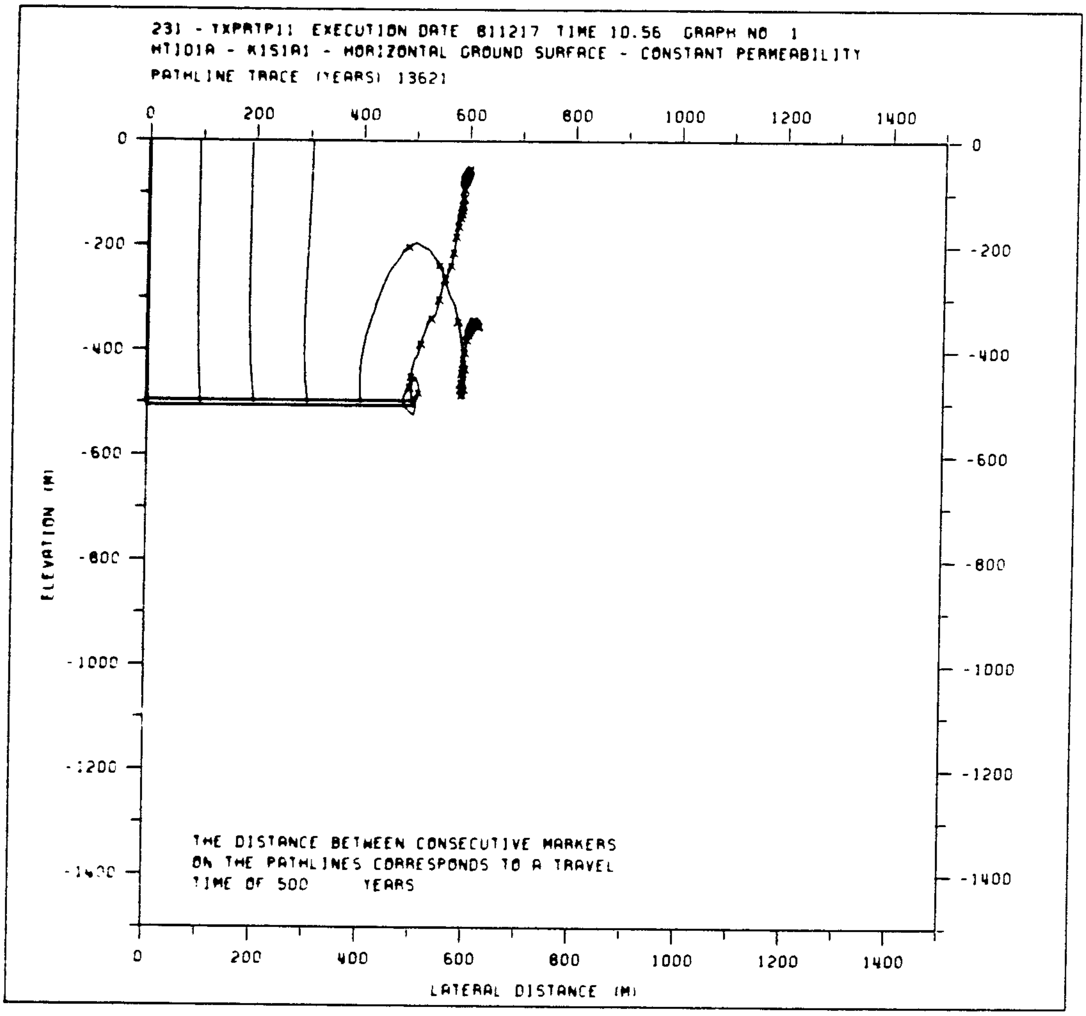


Figure 4.1.1 Pathlines for the fluid flow induced by a radioactive waste repository located below a horizontal ground surface. Permeability and porosity are constant. Vertical anisotropy.

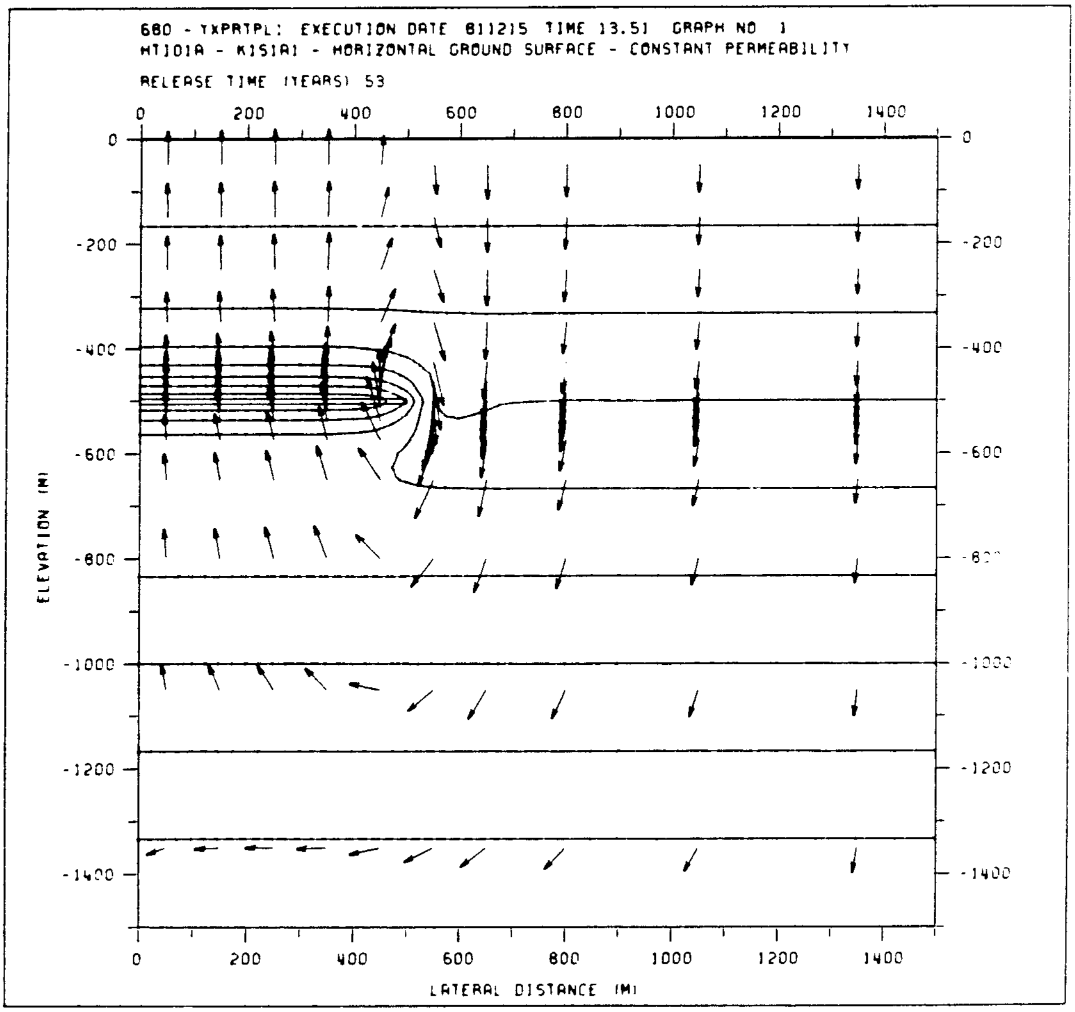


Figure 4.1.2 Groundwater fluxes and isotherms illustrating the hydrothermal flow conditions around a radioactive waste repository situated below a horizontal ground surface. Permeability and porosity are constant. Vertical anisotropy. Release time: 53 years.

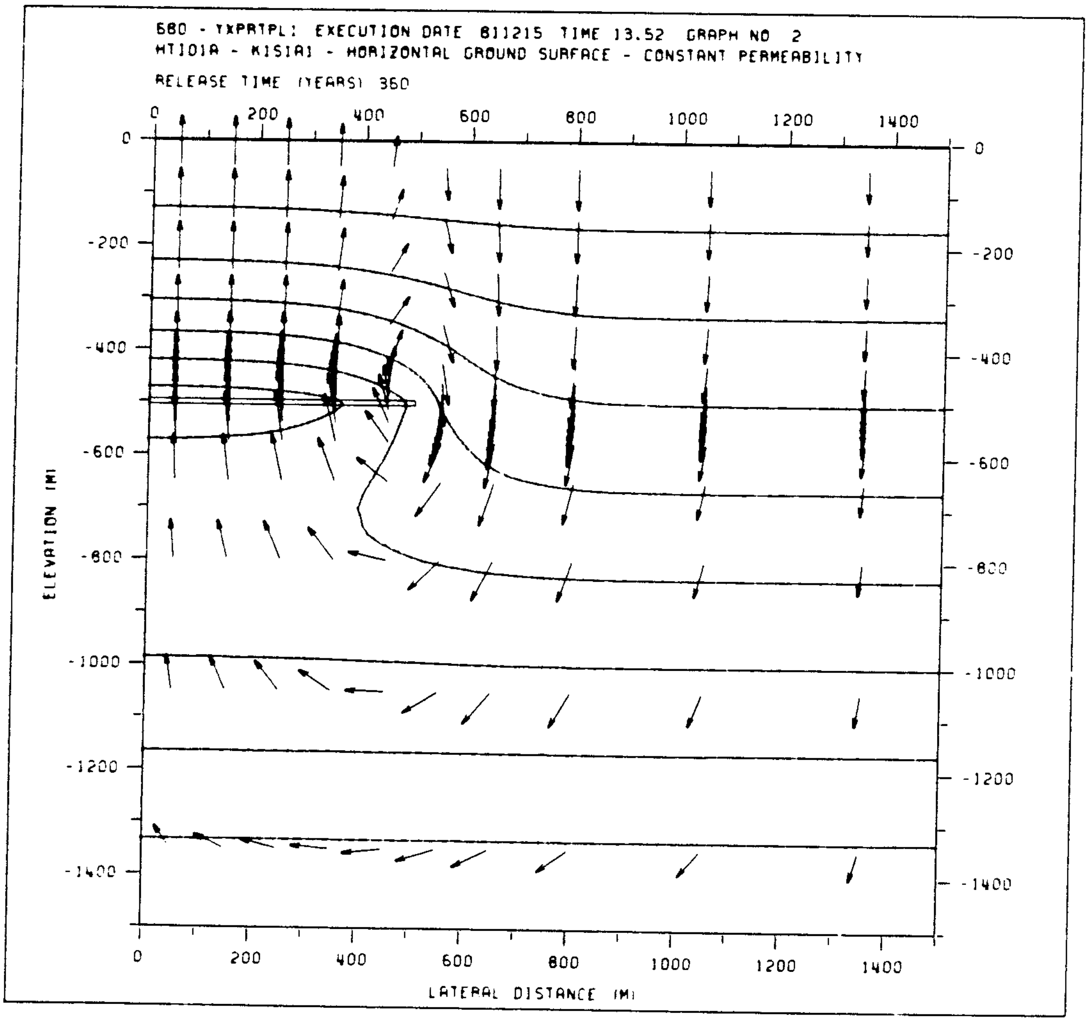


Figure 4.1.3 Groundwater fluxes and isotherms illustrating the hydrothermal flow conditions around a radioactive waste repository situated below a horizontal ground surface. Permeability and porosity are constant. Vertical anisotropy. Release time: 360 years.

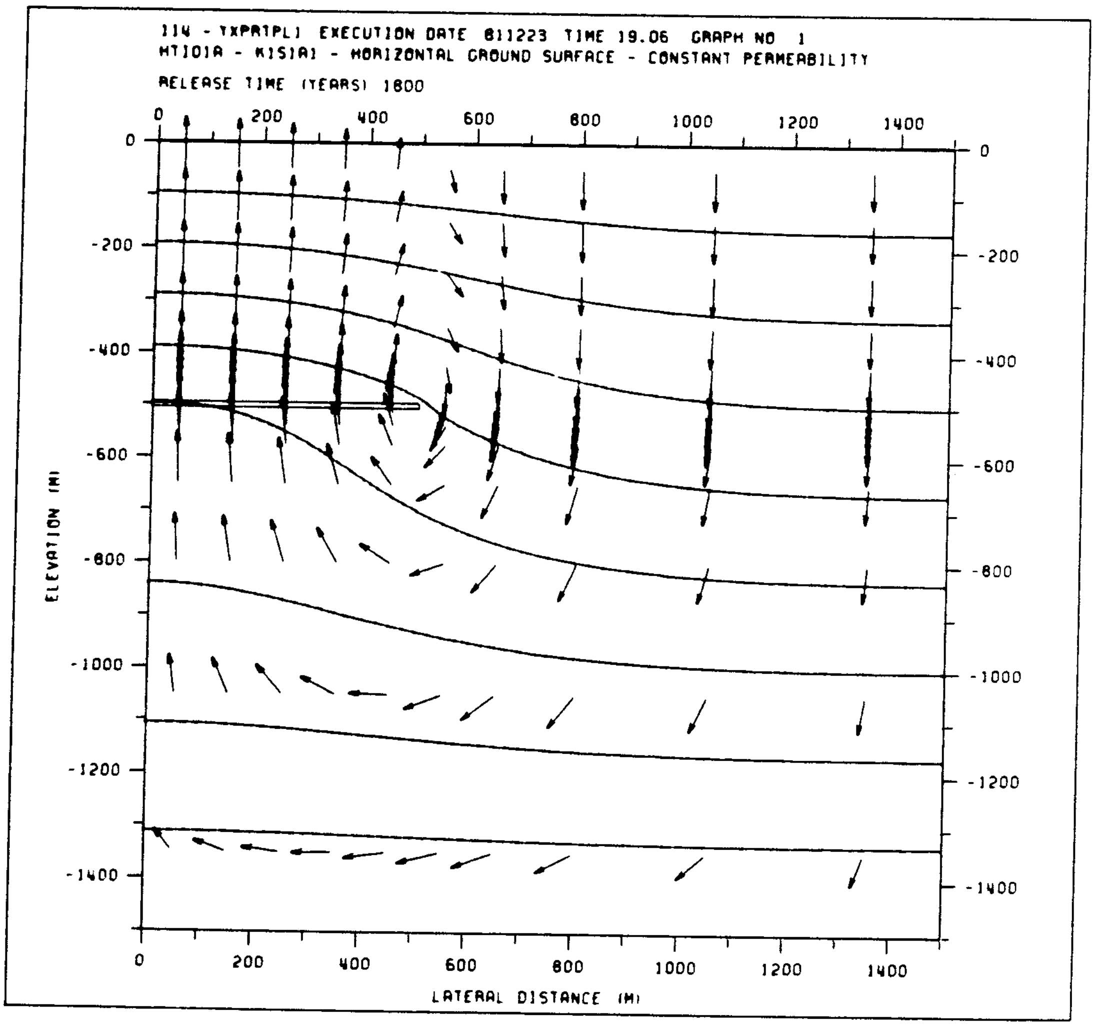


Figure 4.1.4 Groundwater fluxes and isotherms illustrating the hydrothermal flow conditions around a radioactive waste repository situated below a horizontal ground surface. Permeability and porosity are constant. Vertical anisotropy. Release time: 1800 years.

4.1.2 Repository located below a horizontal ground surface. Permeability and porosity are constant over the flow domain. Horizontal anisotropy.

Exit time: > 4400 years

The results of the pathline trace are presented in table 4.1.2.

Pathlines are displayed in figure 4.1.5.

Groundwater fluxes and isotherms are displayed in figures 4.1.6 - 4.1.8.

Considerably longer flow times are to be expected in this example in comparison with those obtained from the previous one. The reason for this is that the comparatively low vertical permeability, that is implied when having horizontal anisotropy, generally will hamper the vertical groundwater movements due to the heat from the repository.

In the present example only the water particle released at the centre of the repository will reach the ground surface, and the travel time for this water particle is calculated to be over 4400 years. This is rather a drastic effect, showing that the influence of anisotropy on the travel times is of great significance.

In the initial stage, the groundwater flow pattern is characterized by convection currents whose paths are elliptic in the region around the edge of the repository. The fluxes below and above the repository, of course with the exception of the region near the centre of the repository, are more or less horizontal. As time proceeds, the centre of the convection cell moves downwards, diagonally towards, the lateral boundary. As a consequence, the fluxes are largely vertical at the repository. As can be seen in the graphical displays of the flow patterns most part of the flow domain is affected by the heat released from the repository.

Table 4.1.2 Coordinates of the starting respectively end points and the corresponding travel times in years of path-lines traced from a radioactive waste repository situated below a horizontal ground surface. Permeability and porosity are constant over the flow domain. Horizontal anisotropy.

| No | Starting point | | End point | | Travel time |
|---|---|---|---|---|---|
| 1 | 0 | -500 | 34 | 0 | 4449 |
| 2 | 100 | -500 | - | - | No exit |
| 3 | 200 | -500 | - | - | No exit |
| 4 | 300 | -500 | - | - | No exit |
| 5 | 400 | -500 | - | - | No exit |
| 6 | 500 | -500 | - | - | No exit |

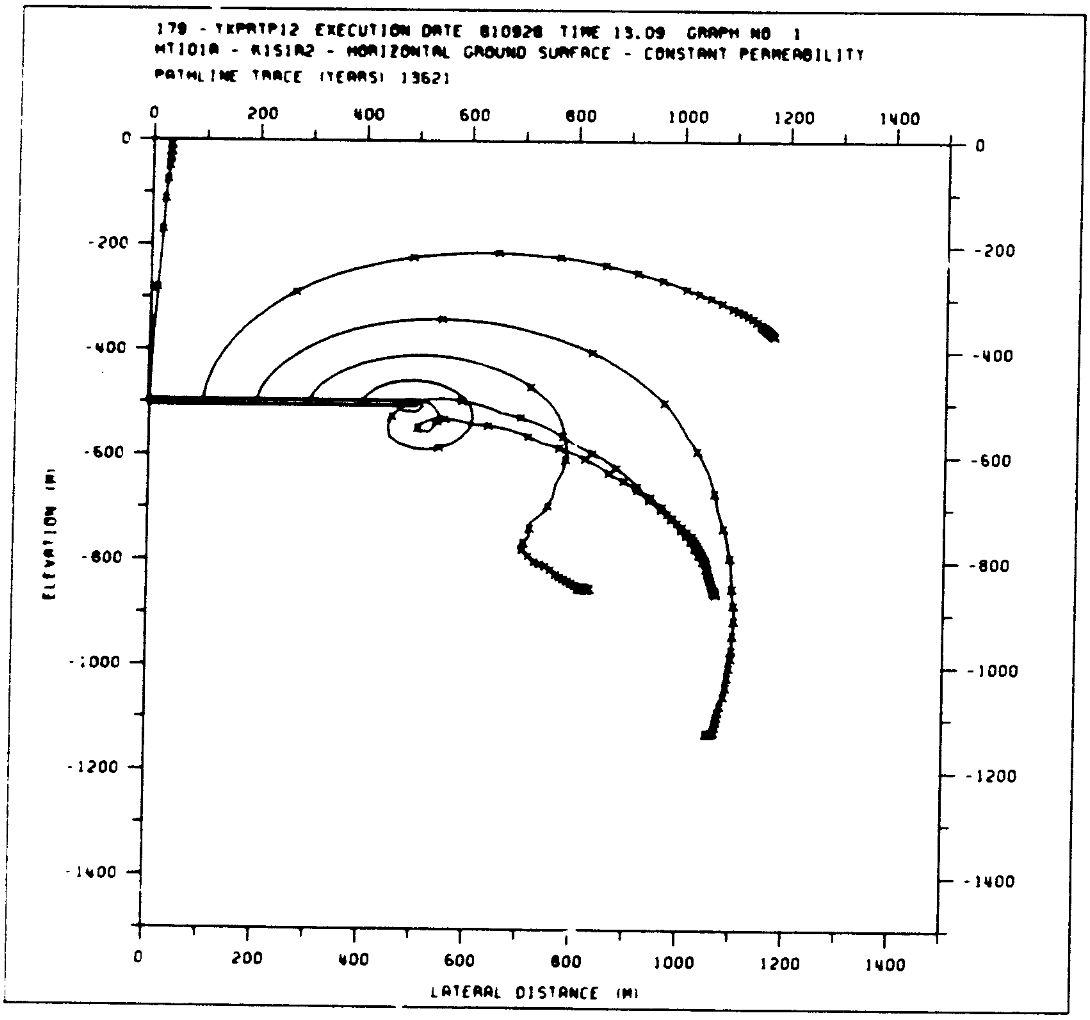


Figure 4.1.5 Pathlines for the fluid flow induced by a radioactive waste repository located below a horizontal ground surface. Permeability and porosity are constant. Horizontal anisotropy.

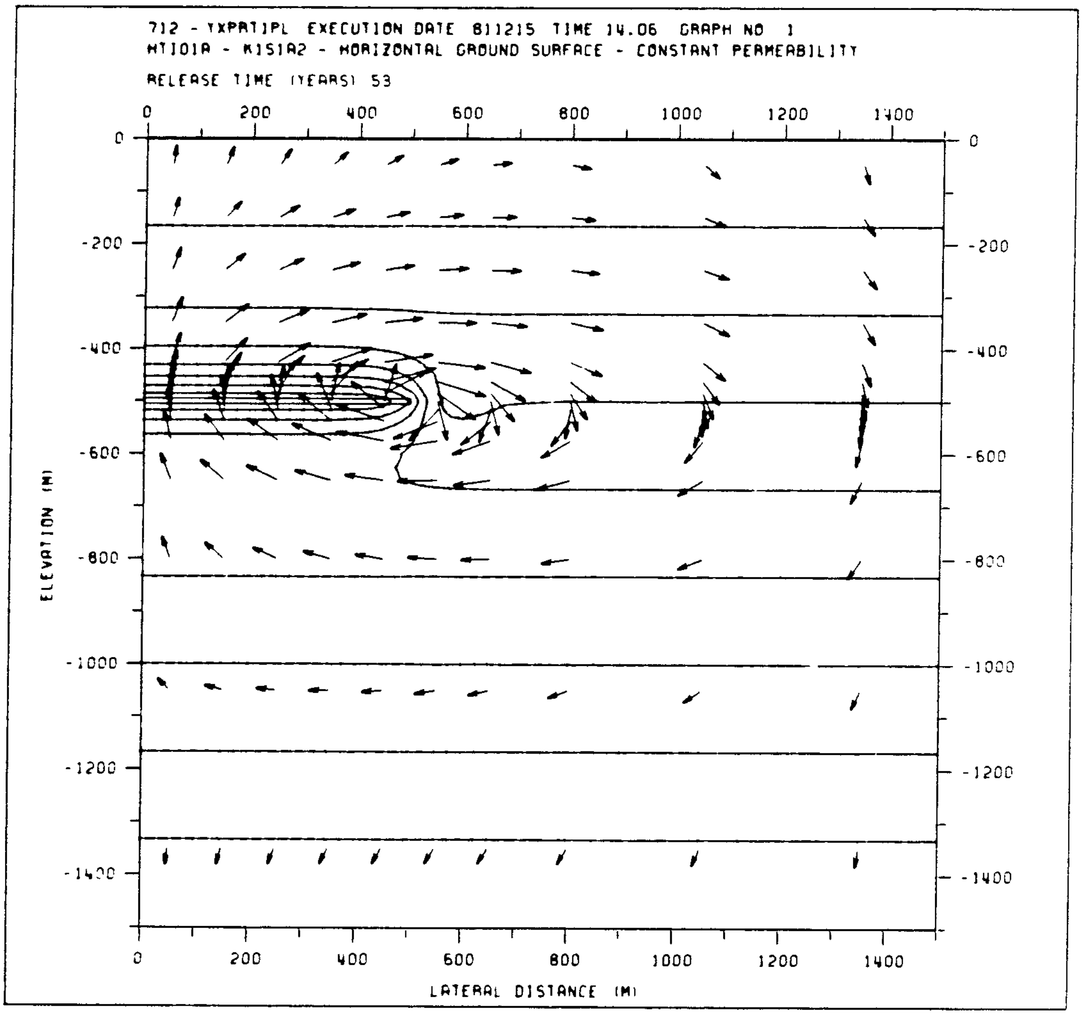


Figure 4.1.6 Groundwater fluxes and isotherms illustrating the hydrothermal flow conditions around a radioactive waste repository situated below a horizontal ground surface. Permeability and porosity are constant. Horizontal anisotropy. Release time: 53 years.

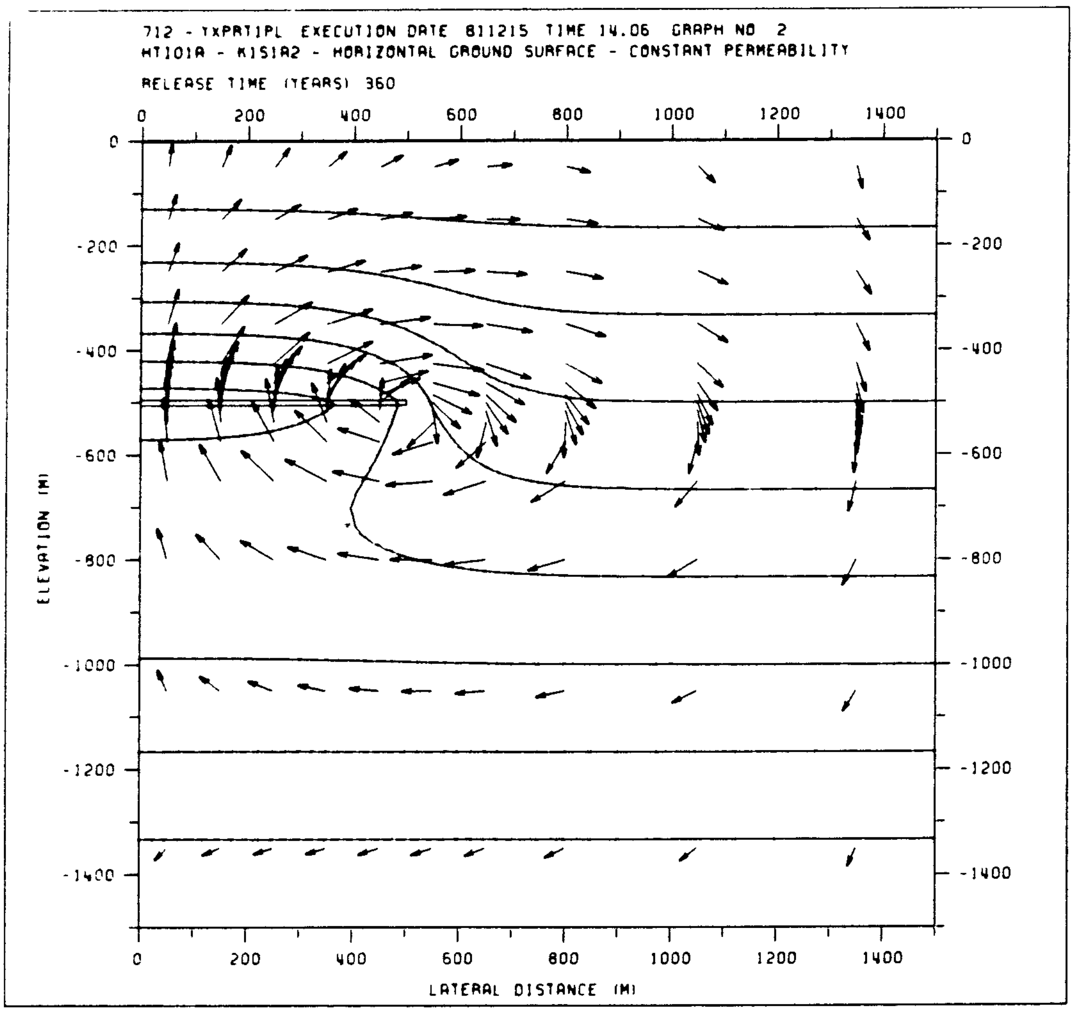


Figure 4.1.7 Groundwater fluxes and isotherms illustrating the hydrothermal flow conditions around a radioactive waste repository situated below a horizontal ground surface. Permeability and porosity are constant. Horizontal anisotropy. Release time: 360 years.

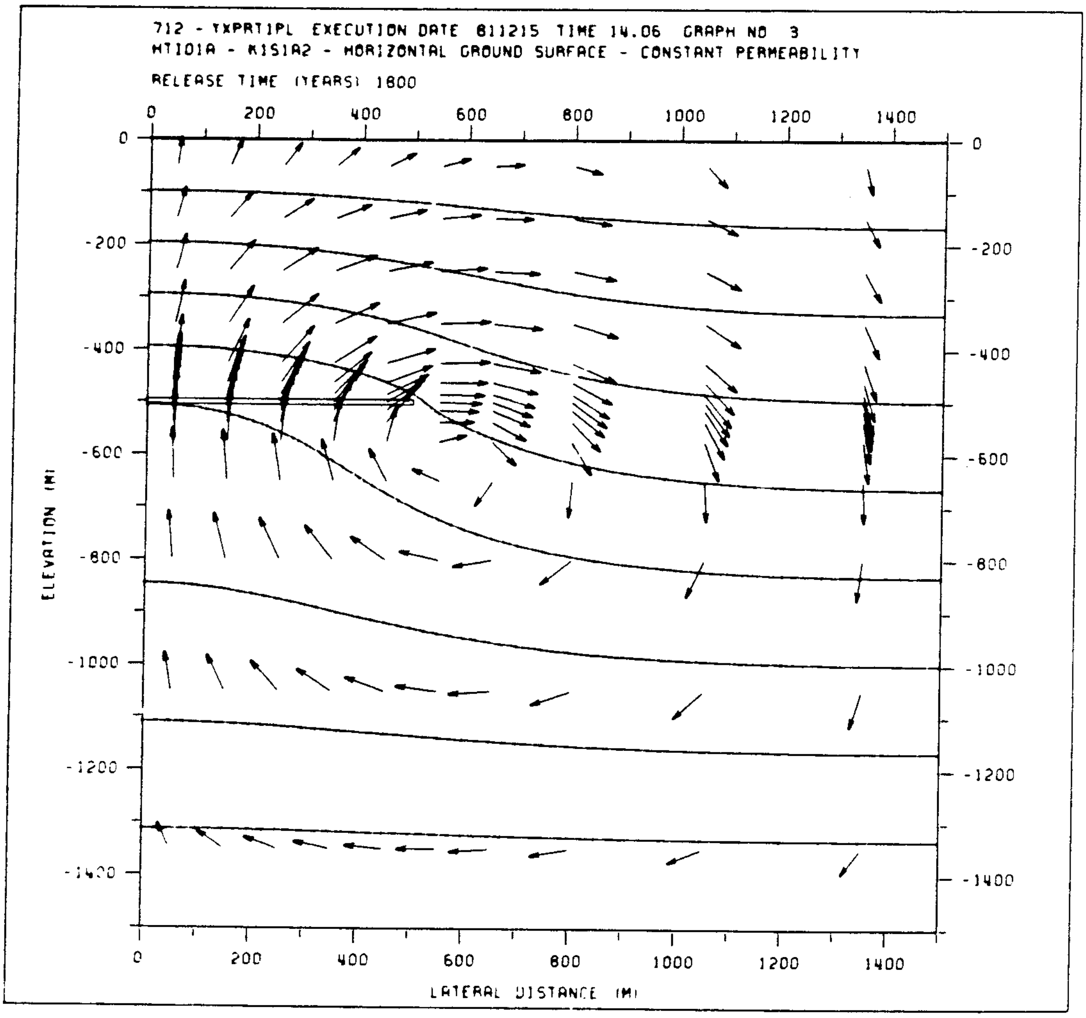


Figure 4.1.8 Groundwater fluxes and isotherms illustrating the hydrothermal flow conditions around a radioactive waste repository situated below a horizontal ground surface. Permeability and porosity are constant. Horizontal anisotropy. Release time: 1800 years.

### 4.1.3 Repository located below a horizontal ground surface. Permeability and porosity decrease exponentially with depth. Vertical anisotropy.

Exit time: No exit

The results of the pathline trace are presented in table 4.1.3.

Pathlines are displayed in figure 4.1.9.

Groundwater fluxes and isotherms are displayed in figures 4.1.10 - 4.1.12.

In this example, the results of the calculations show that the decrease in permeability and porosity with depth over the flow domain has great influence on the travel times. Thus, the very low permeability at great depth, not only governs the flow velocities in the deeper flow regions, but also the flow velocities in the more shallow regions. In consequence of the long flow times, the effect of the heat, being the only cause of the groundwater movements in the present example, vanishes before any water particles will reach the ground surface.

Table 4.1.3 Coordinates of the starting respectively end points and the corresponding travel times in years of pathlines traced from a radioactive waste repository situated below a horizontal ground surface. Permeability and porosity decrease exponentially with depth. Vertical anisotropy.

| No | Starting point | | End point | | Travel time |
|---|---|---|---|---|---|
| 1 | 0 | -500 | 0 | -325 | No exit |
| 2 | 100 | -500 | 42 | -291 | No exit |
| 3 | 200 | -500 | 85 | -279 | No exit |
| 4 | 300 | -500 | 145 | -265 | No exit |
| 5 | 400 | -500 | 212 | -259 | No exit |
| 6 | 500 | -500 | 232 | -275 | No exit |

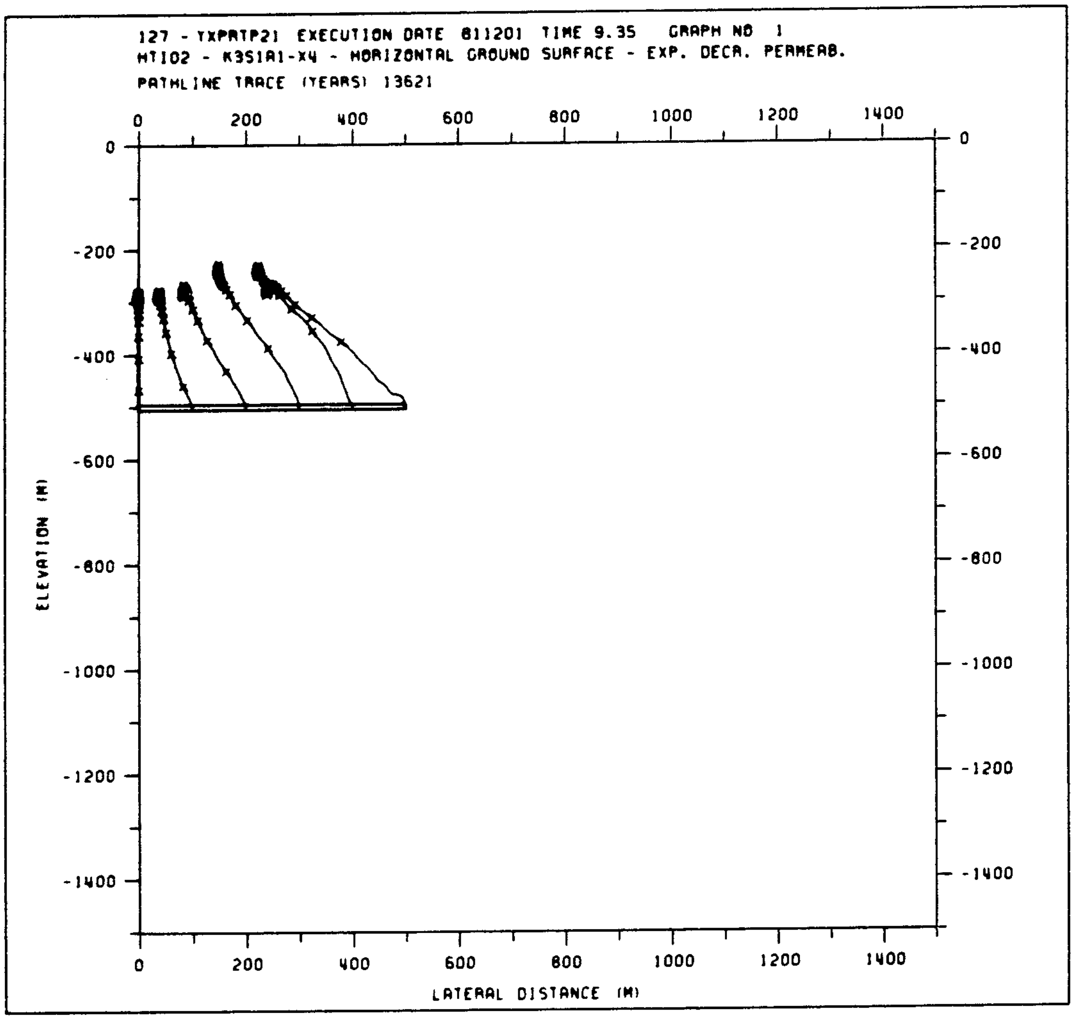


Figure 4.1.9 Pathlines for the fluid flow induced by a radioactive waste repository located below a horizontal ground surface. Permeability and porosity decrease exponentially with depth. Vertical anisotropy.

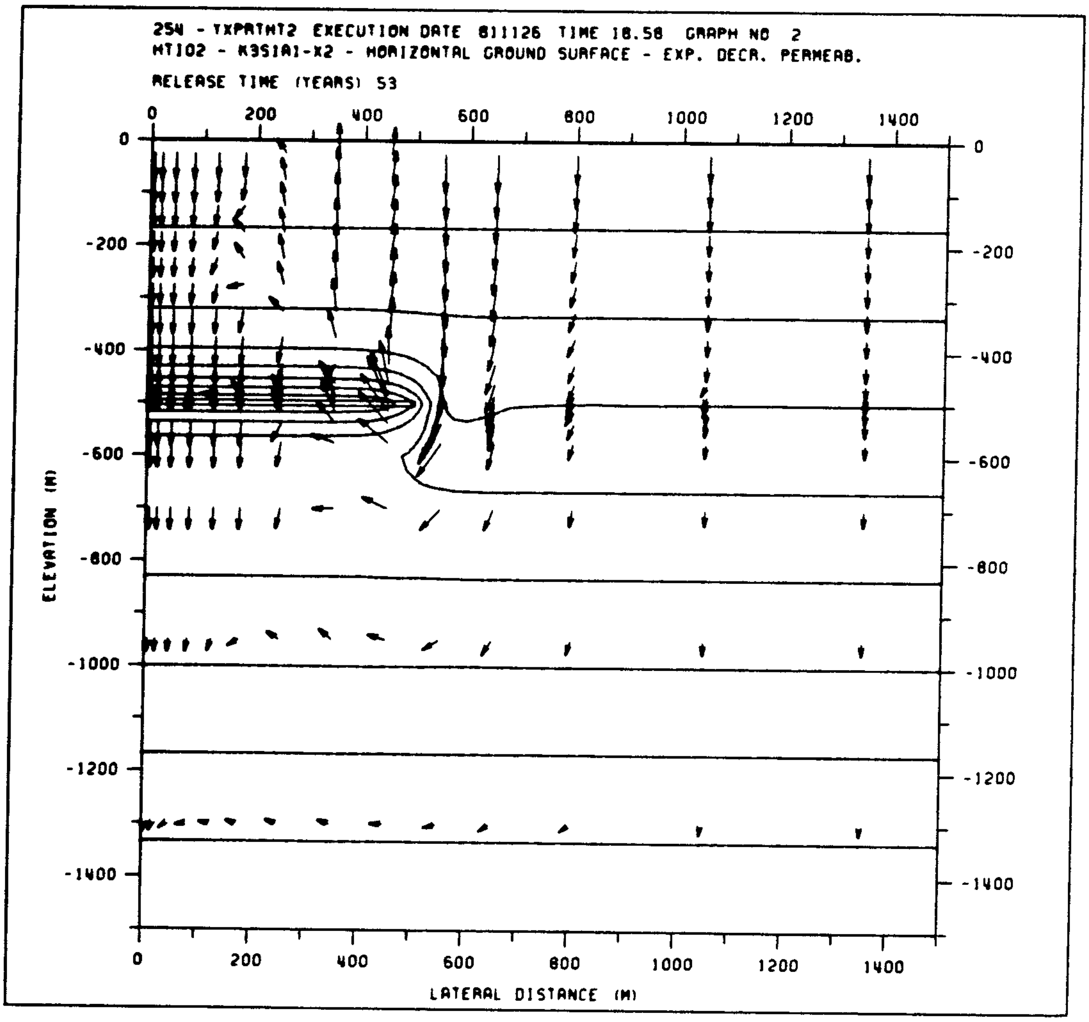


Figure 4.1.10 Groundwater fluxes and isotherms illustrating the hydrothermal flow conditions around a radioactive waste repository situated below a horizontal ground surface. Permeability and porosity decrease exponentially with depth. Vertical anisotropy. Release time: 53 years.

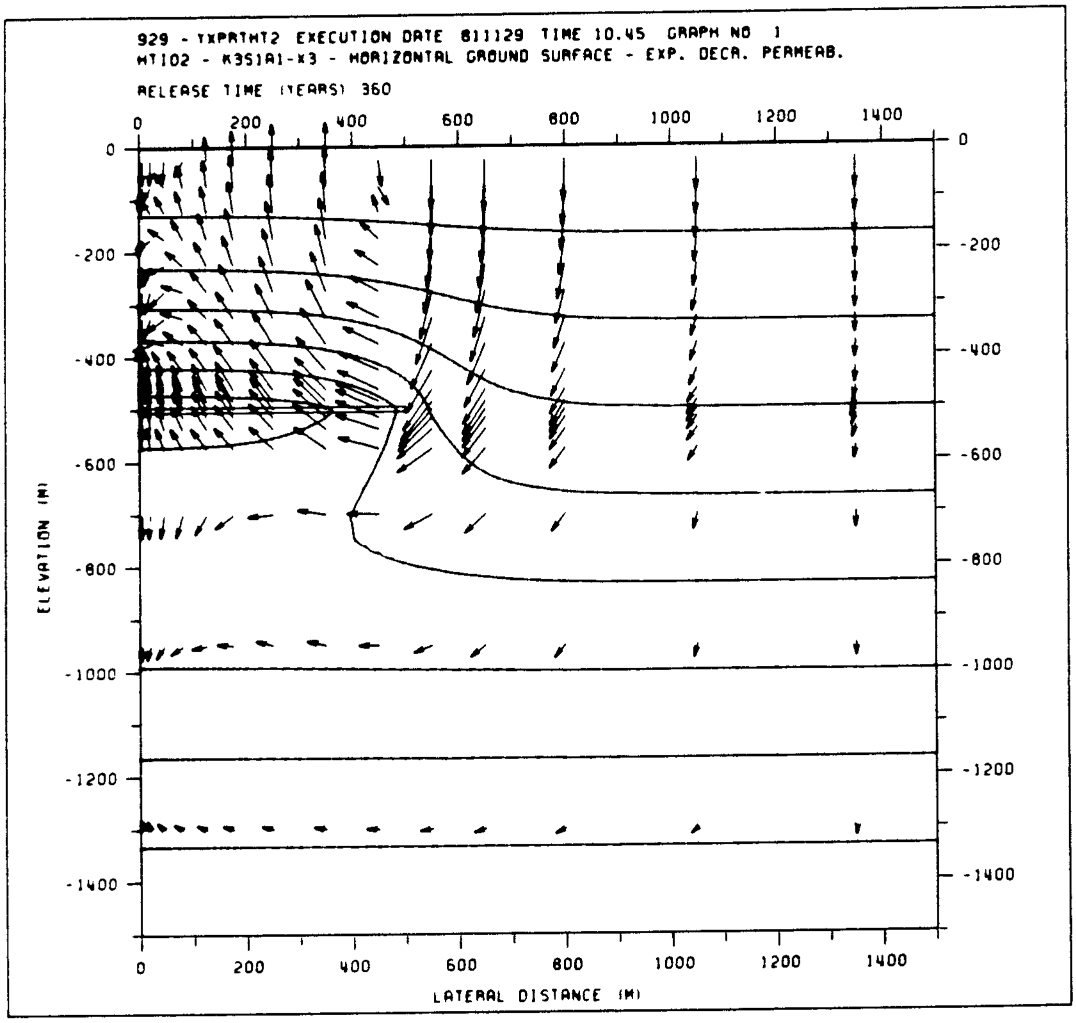


Figure 4.1.11 Groundwater fluxes and isotherms illustrating the hydrothermal flow conditions around a radioactive waste repository situated below a horizontal ground surface. Permeability and porosity decrease exponentially with depth. Vertical anisotropy. Release time: 360 years.

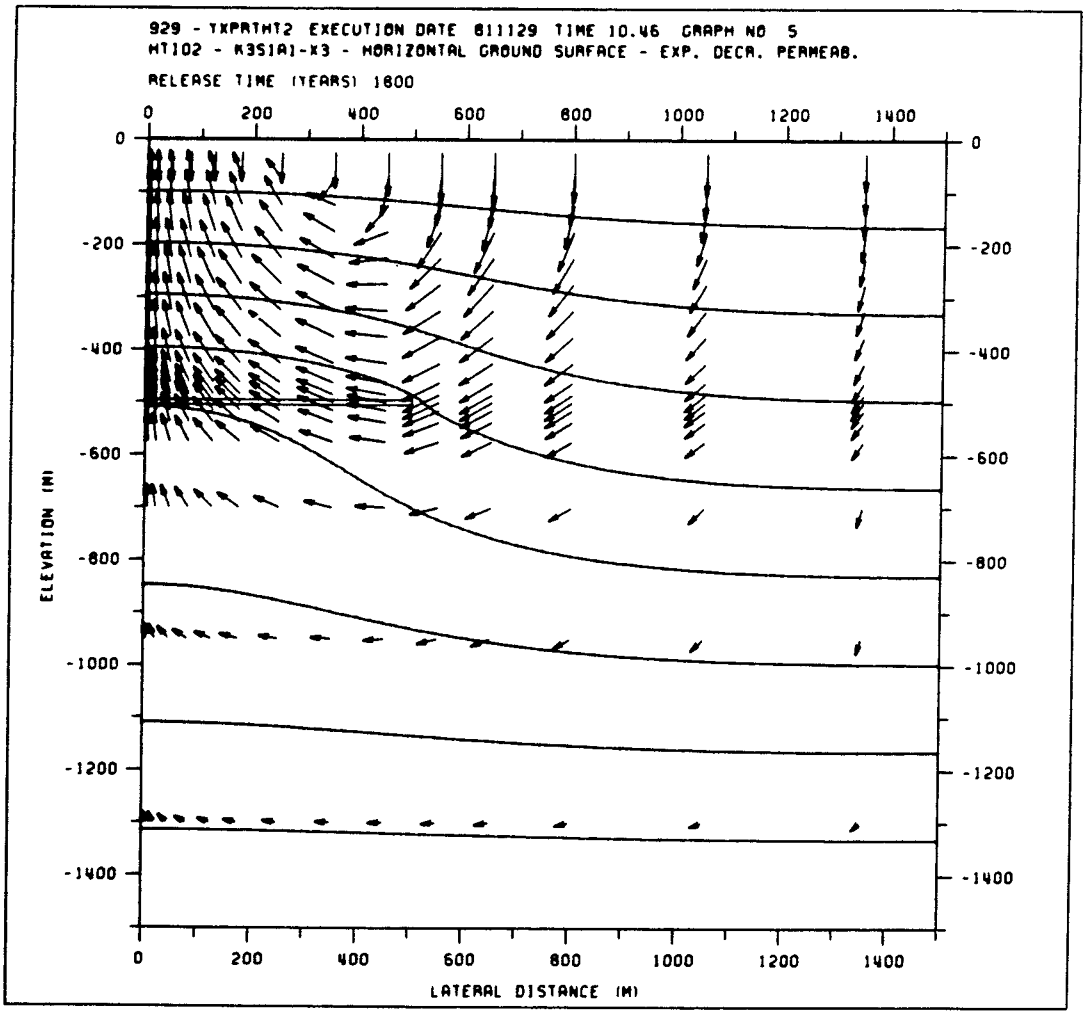


Figure 4.1.12 Groundwater fluxes and isotherms illustrating the hydrothermal flow conditions around a radioactive waste repository situated below a horizontal ground surface. Permeability and porosity decrease exponentially with depth. Vertical anisotropy. Release time: 1800 years.

### 4.1.4 Repository located below a horizontal ground surface. Permeability and porosity decrease exponentially with depth. Horizontal anisotropy.

Exit time: No exit

The results of the pathline trace are presented in table 4.1.4.

Pathlines are displayed in figure 4.1.13.

Groundwater fluxes and isotherms are displayed in figures 4.1.14 - 4.1.16.

As in the previous example with vertical anisotropy, none of the traced water particles will reach the ground surface. A notable difference is, however, that the water particles traced from the repository are stopping more close to the ground surface in the present example than in the previous one.

At the beginning, the centre of the rotative movement, induced by the heat from the repository, is located at the edge of the repository. After about two thousand years, the centre of the rotative movements is moved upwards, towards the ground surface, to a depth of about 200 metres below the ground surface. As a result, the groundwater fluxes become horizontal at the edges of the repository. Furthermore, the groundwater fluxes in the region below the repository are extremely small in comparison with the fluxes in the region above the repository.

Table 4.1.4 Coordinates of the starting respectively end points and the corresponding travel times in years of path-lines traced from a radioactive waste repository situated below a horizontal ground surface. Permeability and porosity decrease exponentially with depth. Horizontal anisotropy.

| No | Starting point | | End point | | Travel time |
|---|---|---|---|---|---|
| 1 | 0 | -500 | 0 | -138 | No exit |
| 2 | 100 | -500 | 54 | -137 | No exit |
| 3 | 200 | -500 | 114 | -142 | No exit |
| 4 | 300 | -500 | 178 | -151 | No exit |
| 5 | 400 | -500 | 232 | -164 | No exit |
| 6 | 500 | -500 | 215 | -164 | No exit |

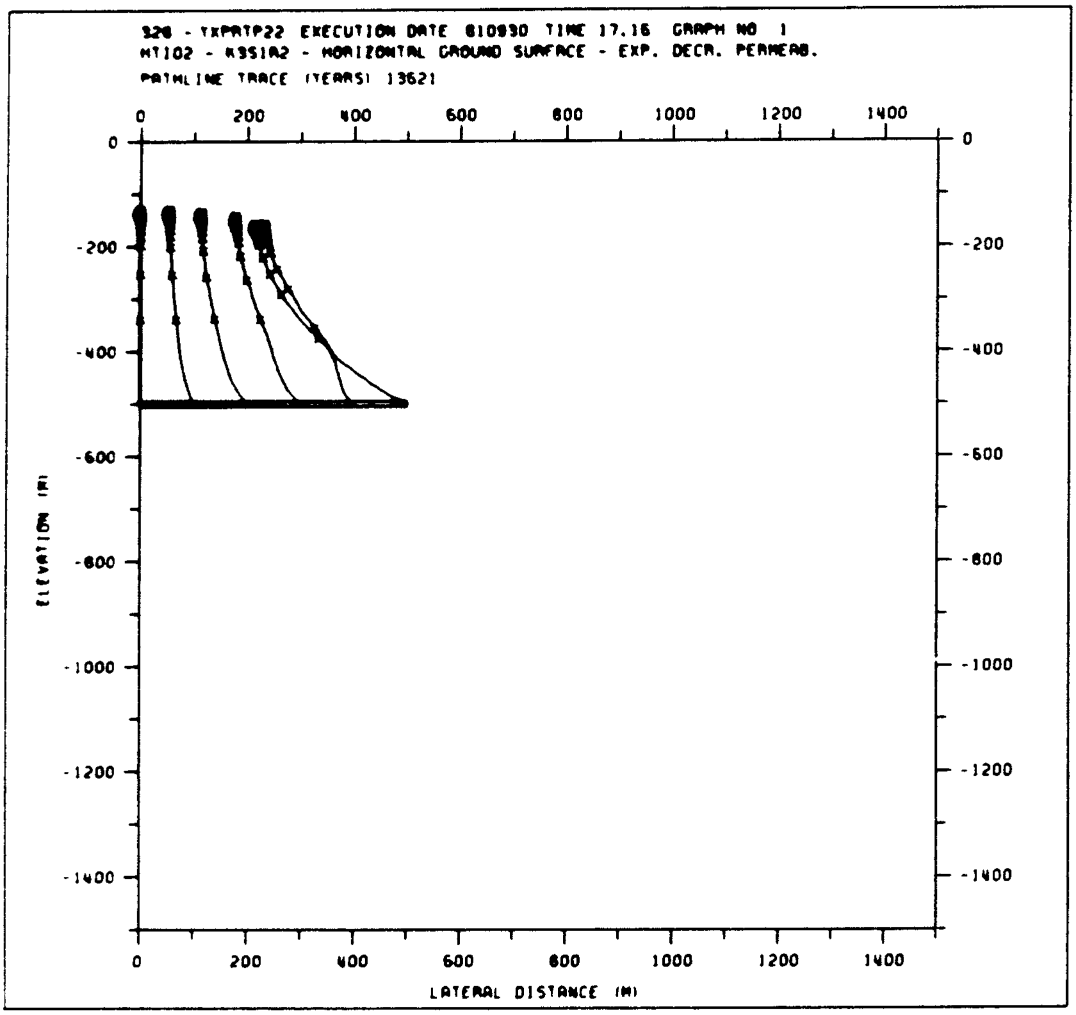


Figure 4.1.13 Pathlines for the fluid flow induced by a radioactive waste repository located below a horizontal ground surface. Permeability and porosity decrease exponentially with depth. Horizontal anisotropy.

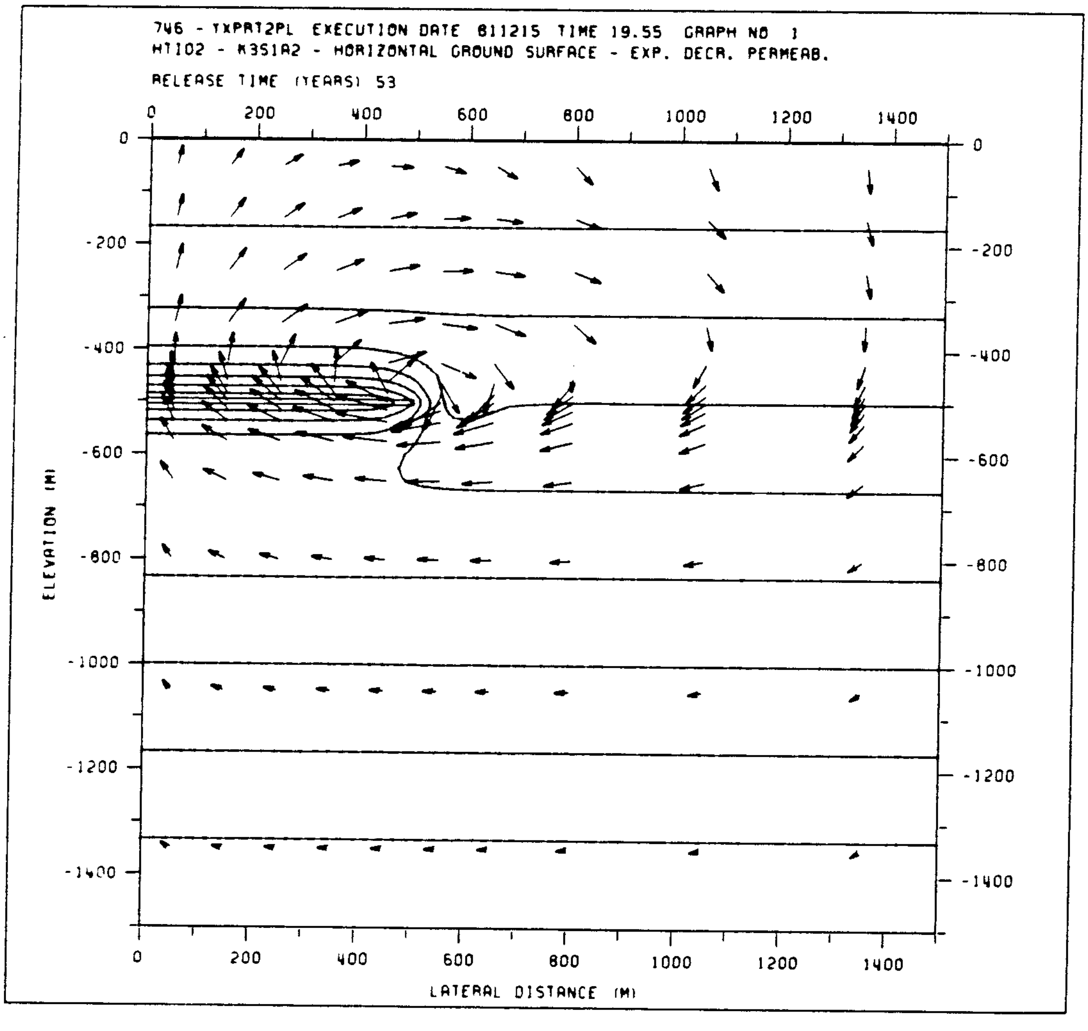


Figure 4.1.14 Groundwater fluxes and isotherms illustrating the hydrothermal flow conditions around a radioactive waste repository situated below a horizontal ground surface. Permeability and porosity decrease exponentially with depth. Horizontal anisotropy. Release time: 53 years.

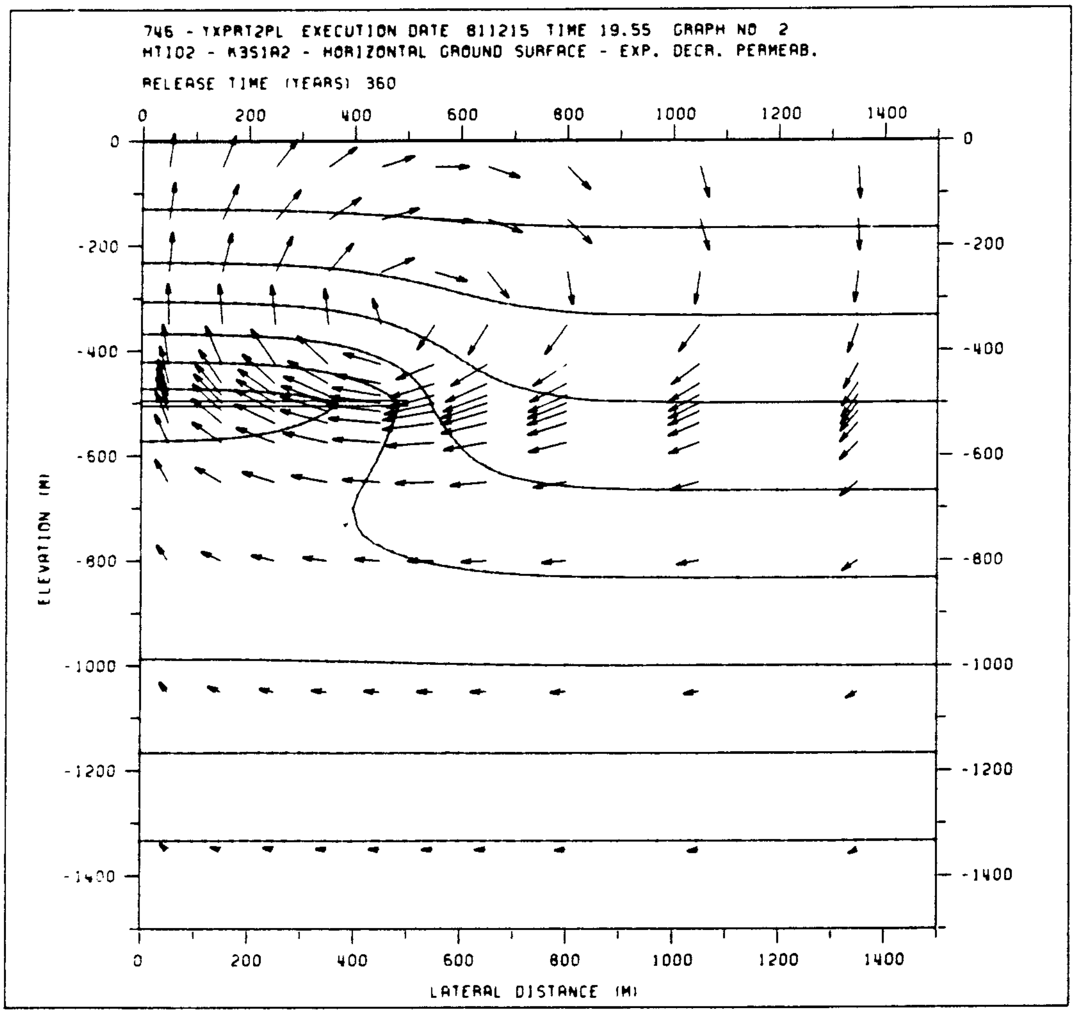


Figure 4.1.15 Groundwater fluxes and isotherms illustrating the hydrothermal flow conditions around a radioactive waste repository situated below a horizontal ground surface. Permeability and porosity decrease exponentially with depth. Horizontal anisotropy. Release time: 360 years.

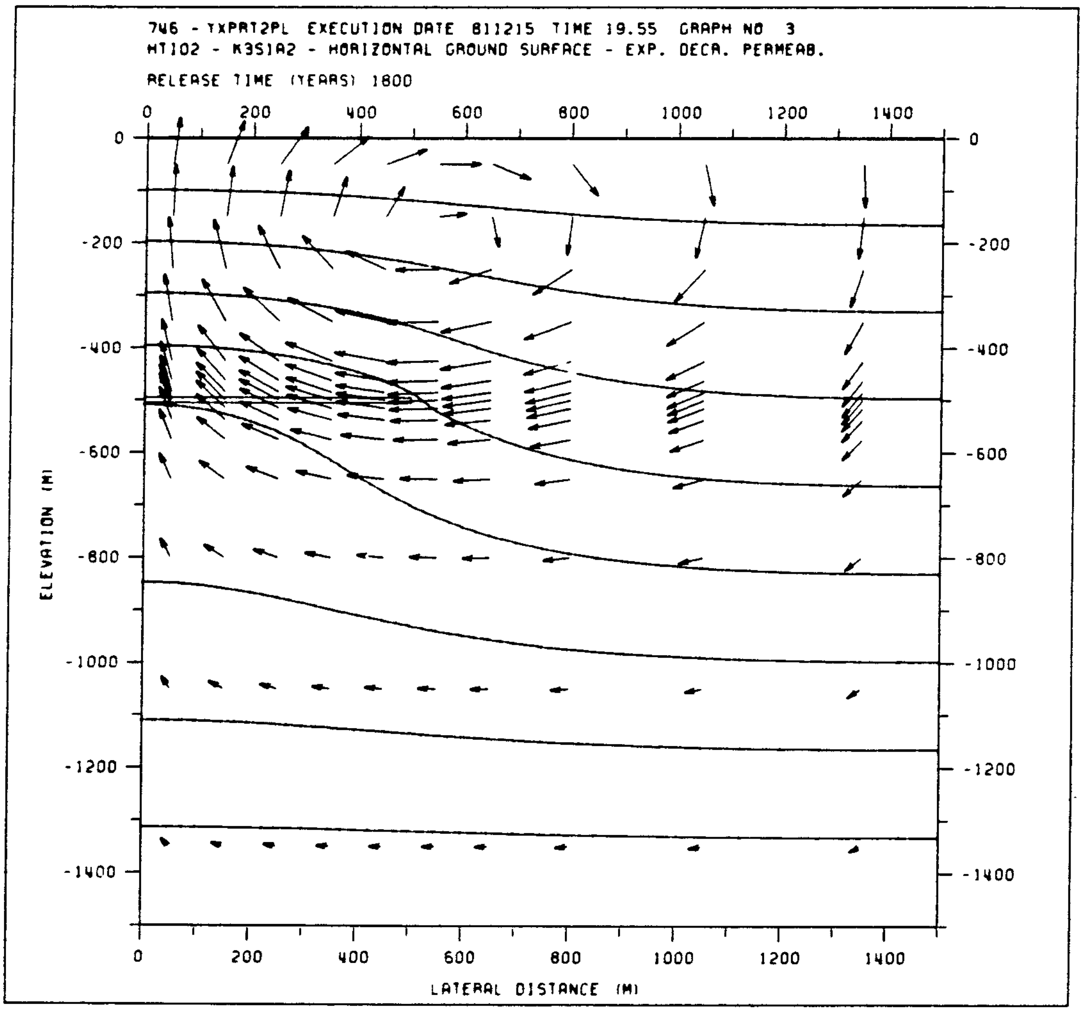


Figure 4.1.16 Groundwater fluxes and isotherms illustrating the hydrothermal flow conditions around a radioactive waste repository situated below a horizontal ground surface. Permeability and porosity decrease exponentially with depth. Horizontal anisotropy. Release time: 1800 years.

## 4.2 Repository located below the crest of a hill

The repository is symmetrically located below the crest of the hill, and the hillsides are assumed to slope linearly in each direction. In this case the groundwater flow is induced both by the sloping ground surface and by the heat released from the repository. The behaviour of this problem is much more difficult to tell beforehand than that of the previous one. This is due to the fact that the influence of the heat upon the groundwater movements is varying with time.

At the beginning, the flow is governed by the topographical gradients only. Then, some time after the emplacement of the waste, there is a period when the heat released from the repository is exerting significance influence on the flow pattern. Thus, the flow pattern is affected by the heat from the repository for some thousand years, before the flow conditions begin reverting to the initial ones.

Four examples are worked out for this case and they are organized as follows:

4.2.1 Repository located below the crest of a hill with a slope of one per mille. Constant permeability and porosity and vertical anisotropy in permeability.

4.2.2 Repository located below the crest of a hill with a slope of one per mille. Constant permeability and porosity and horizontal anisotropy in permeability.

4.2.3 Repository located below the crest of a hill with a slope of one per mille. Exponentially decreasing permeability and porosity with depth and vertical anisotropy in permeability.

4.2.4 Repository located below the crest of a hill with a slope of one per mille. Exponentially decreasing permeability and porosity with depth and horizontal anisotropy in permeability.

The presentation of these examples is similar to that of the previous set of examples, in which the ground surface was horizontal. However, in the present analysis it is of great interest to obtain travel times as well as pathlines, also without the influence of the heat from the repository, implying that the groundwater flow is governed by the topographical gradients only.

In these examples the inflow area is situated at the crest of the hill above the repository, and the outflow area is situated at the lateral boundary. As in the previous case, it is assumed that the water level is constant with time. This implies, that the recharge at the inflow area is sufficient to maintain the water table at the crest of the hill, and that the water being discharged at the outflow area is removed by some process. Groundwater fluxes are displayed in the form of vectors and temperatures in the form of isotherms at the following times after the emplacement of the radioactive waste: 0, 53, 360 and 1800 years.

### 4.2.1 Repository located below the crest of a hill with a slope of one per mille. Permeability and porosity are constant. Vertical anisotropy.

Exit time: > 1000 years

> 3000 years without the influence of a repository

The results of the pathline trace are presented in tables 4.2.1 and 4.2.2.

Pathlines for the flow conditions with the influence of a repository are displayed in figure 4.2.1.

Pathlines for the natural flow conditions without the influence of a repository are displayed in figure 4.2.2.

Groundwater fluxes and isotherms are displayed in figures 4.2.3 - 4.2.6.

The effect of vertical anisotropy in the present example is to enhance the uplift, caused by the heat from the repository, of water particles flowing from the repository. Thus, the water particle starting at a distance of 100 metres from the centre of the repository will reach the ground surface already after about 1000 years. In a previous investigation the shortest travel time for isotropic flow conditions was calculated to be about 3800 years. Water particles starting near the edges of the repository are getting involved in the convection currents, created around the edges of the repository. As a result, the travel times for these water particles to reach the ground surface become much longer than the above mentioned travel time for the very first water particle to reach the ground surface.

Table 4.2.1 Coordinates of the starting respectively end points and the corresponding travel times in years of pathlines traced from a radioactive repository located below the crest of a hill with a slope of one per mille. Permeability and porosity are constant over the flow domain. Vertical anisotropy.

| No | Starting point | | End point | | Travel time |
|---|---|---|---|---|---|
| 1 | 0 | -500 | 1365 | 0 | 7834 |
| 2 | 100 | -500 | 311 | 0 | 1074 |
| 3 | 200 | -500 | 1356 | 0 | 4666 |
| 4 | 300 | -500 | 1457 | 0 | 7461 |
| 5 | 400 | -500 | 1387 | 0 | 6534 |
| 6 | 500 | -500 | 1391 | 0 | 6496 |

Table 4.2.2 Coordinates of the starting respectively end points and the corresponding travel times in years of pathlines traced from a repository located below the crest of a hill with a slope of one per mille. Permeability and porosity are constant over the flow domain. Vertical anisotropy. No heat is released from the repository.

| No | Starting point | | End point | | Travel time |
|---|---|---|---|---|---|
| 1 | 0 | -500 | - | - | >11000 |
| 2 | 100 | -500 | 1443 | 0 | 5729 |
| 3 | 200 | -500 | 1388 | 0 | 4680 |
| 4 | 300 | -500 | 1330 | 0 | 3988 |
| 5 | 400 | -500 | 1293 | 0 | 3472 |
| 6 | 500 | -500 | 1255 | 0 | 2975 |

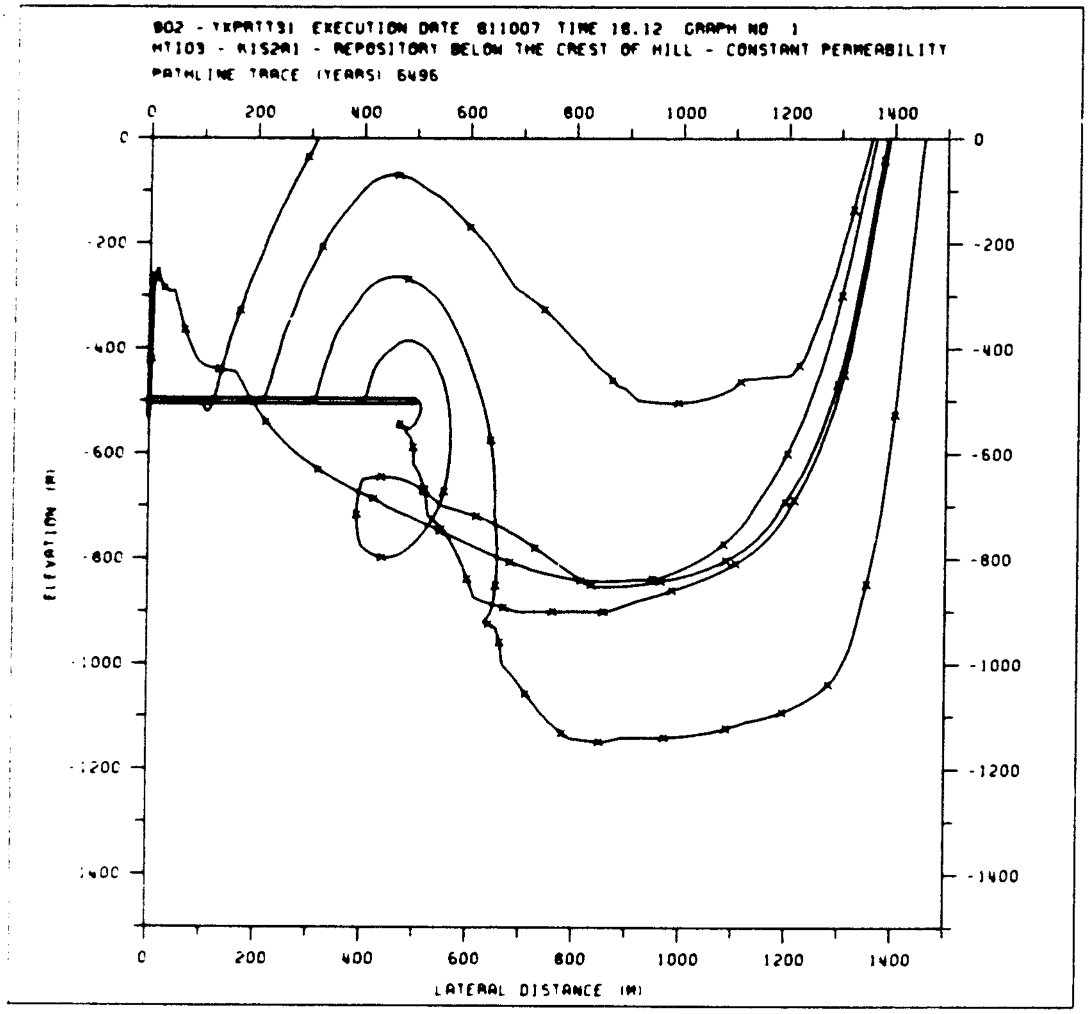


Figure 4.2.1 Pathlines for the flow conditions with the influence of a repository located below the crest of a hill with a slope of the hillsides of one per mille. Permeability and porosity are constant. Vertical anisotropy.

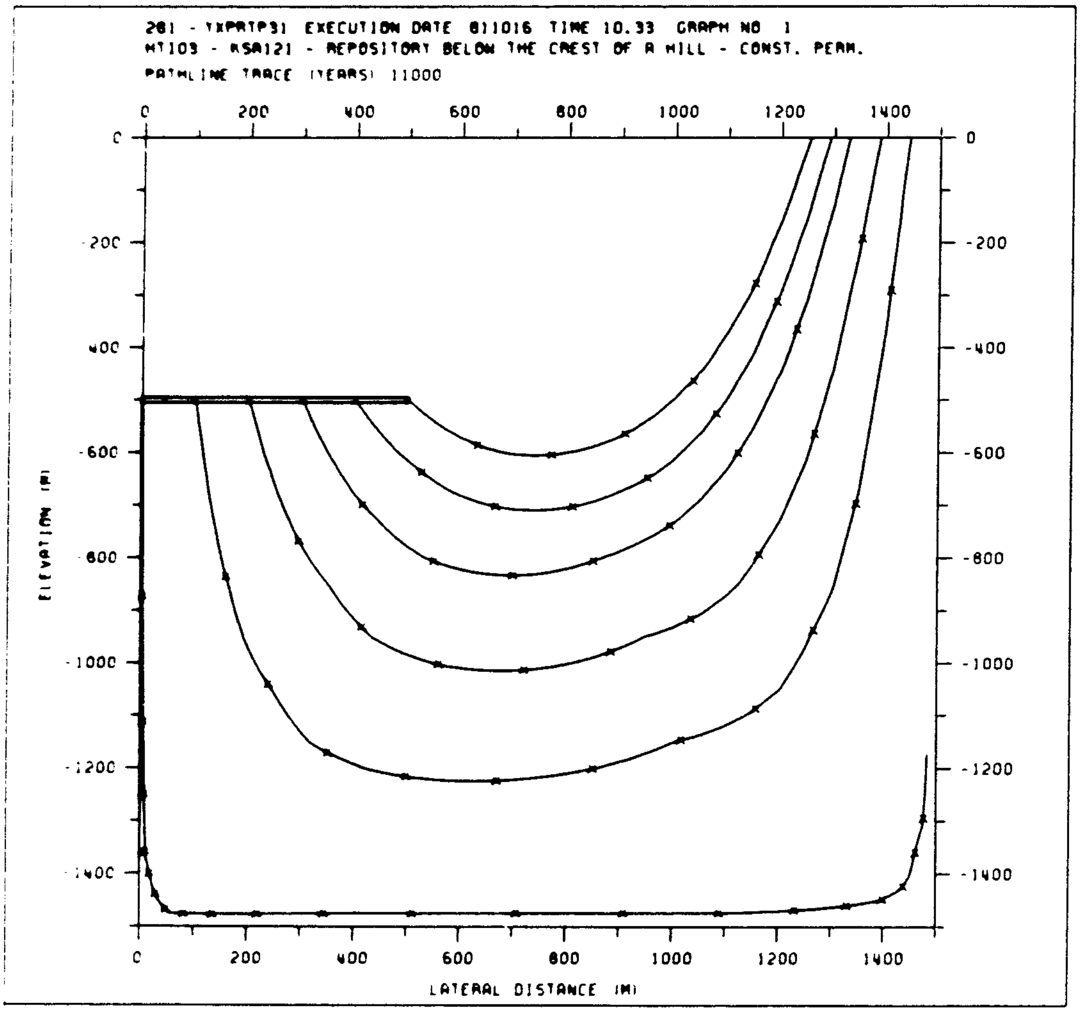


Figure 4.2.2 Pathlines for the natural flow conditions below the crest of a hill with a slope of one per mille. Permeability and porosity are constant. Vertical anisotropy.

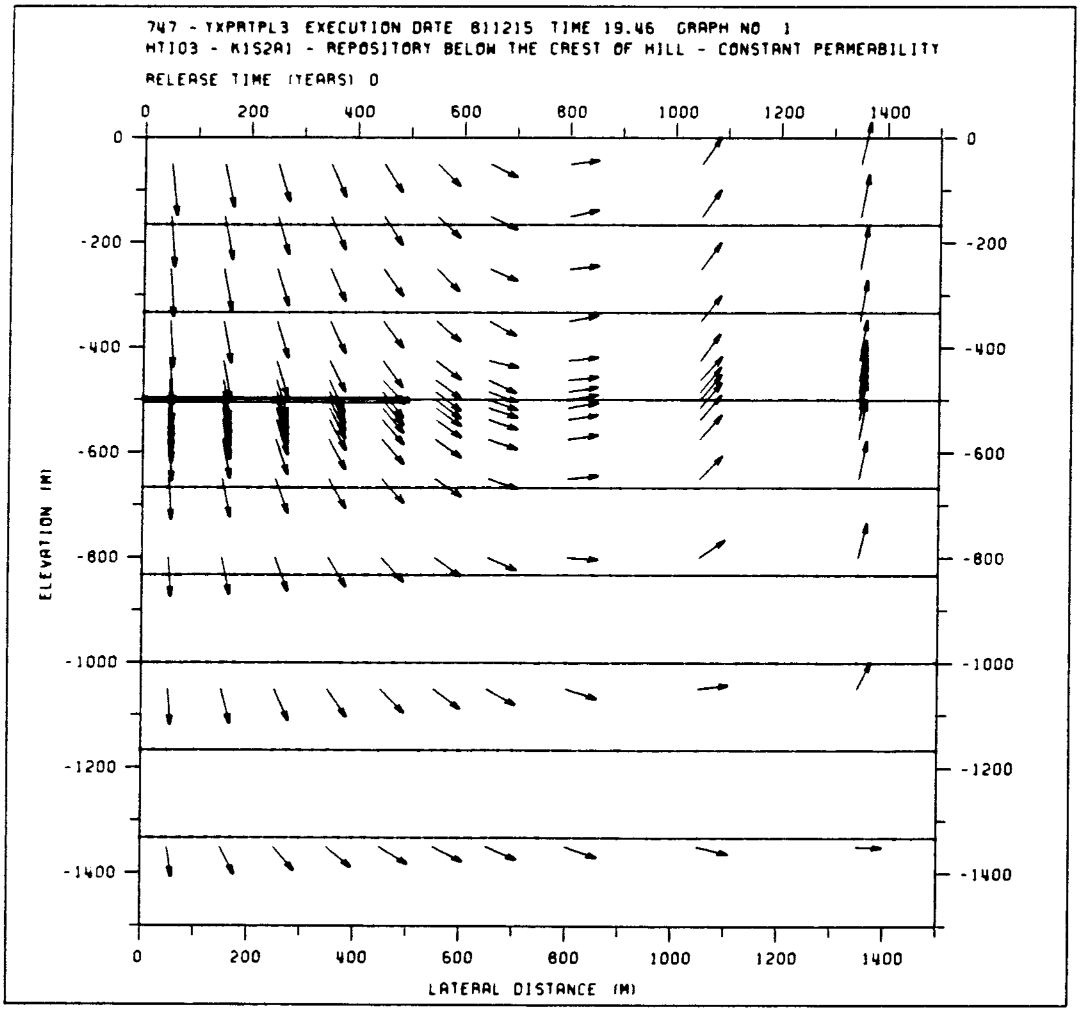


Figure 4.2.3 Groundwater fluxes and isotherms illustrating the hydrothermal flow conditions around a radioactive waste repository situated below the crest of a hill with a slope of one per mille. Permeability and porosity are constant. Vertical anisotropy. Release time: 0 years.

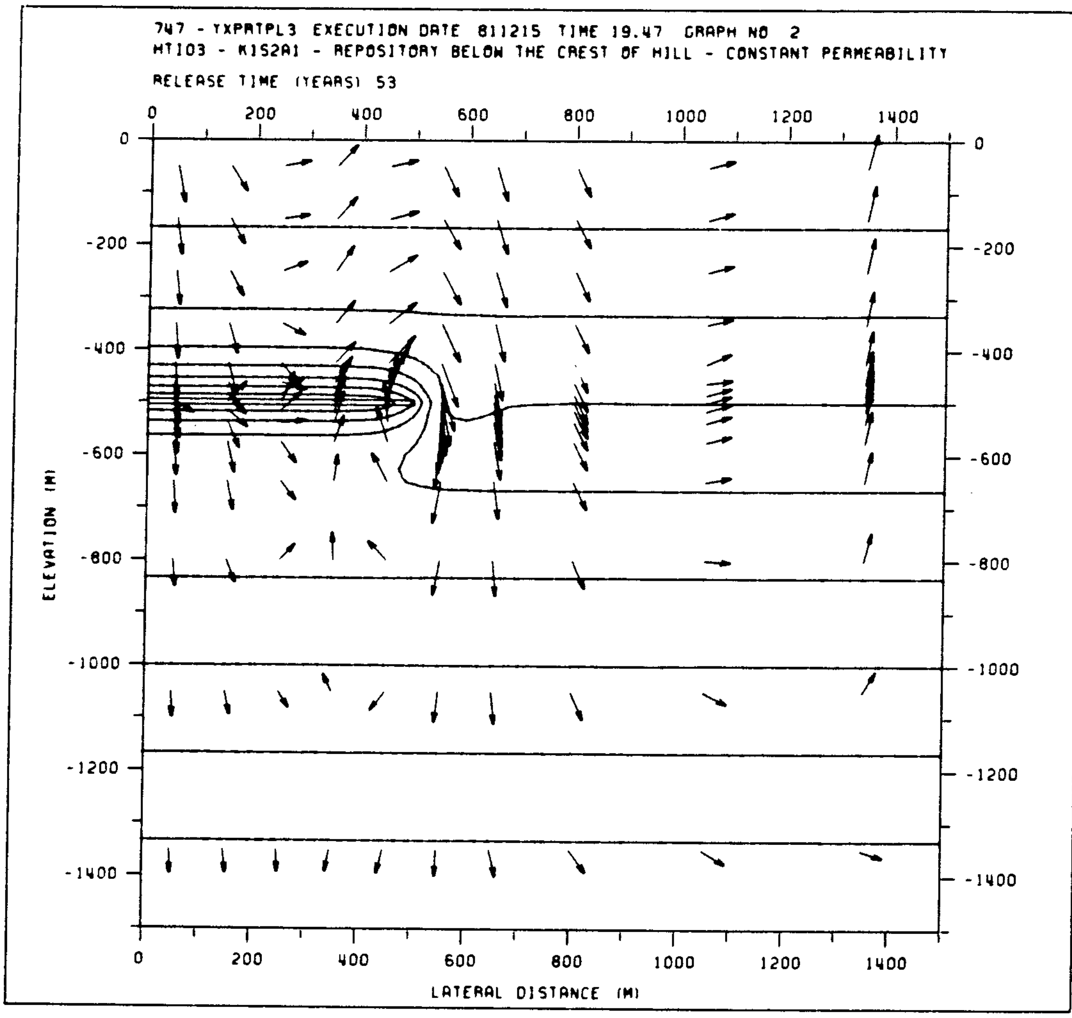


Figure 4.2.4 Groundwater fluxes and isotherms illustrating the hydrothermal flow conditions around a radioactive waste repository situated below the crest of a hill with a slope of one per mille. Permeability and porosity are constant. Vertical anisotropy. Release time: 53 years.

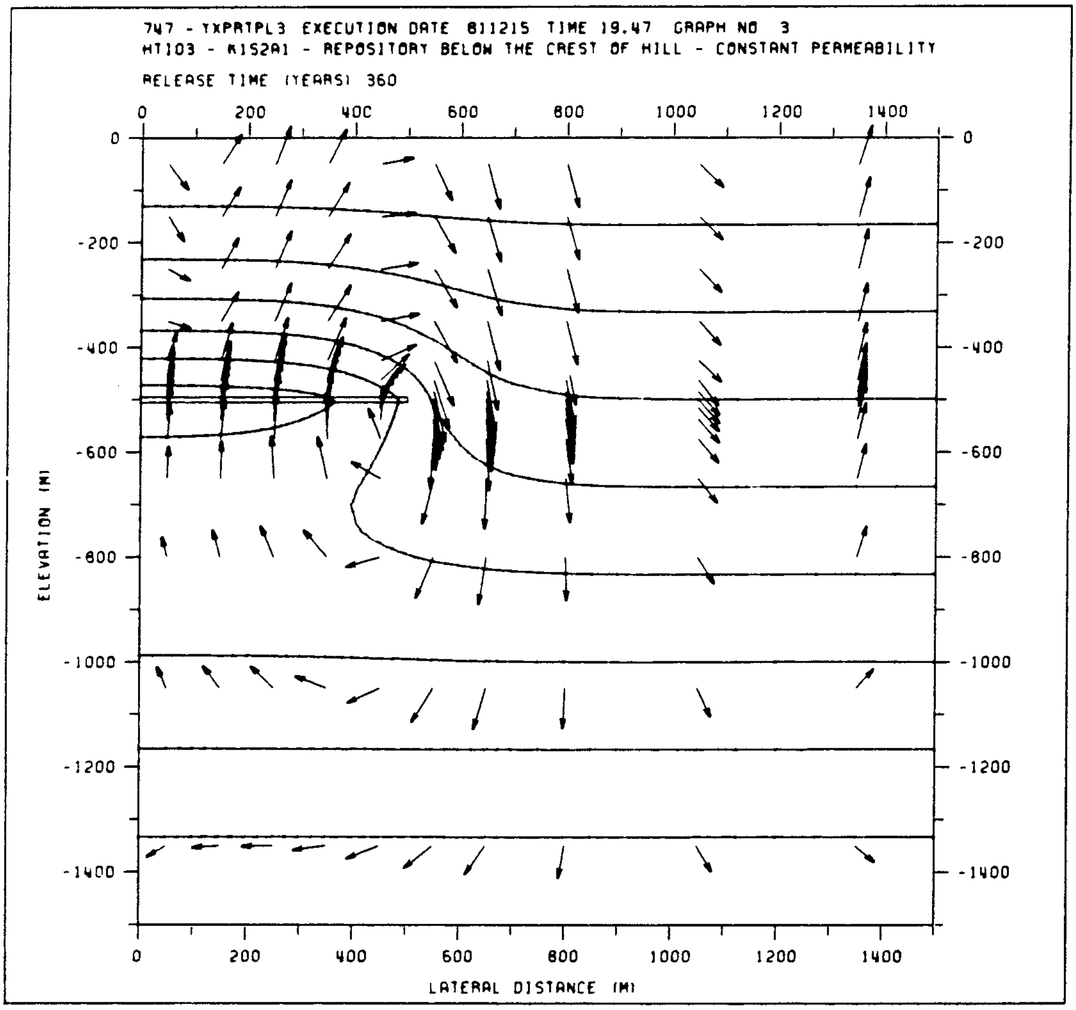


Figure 4.2.5 Groundwater fluxes and isotherms illustrating the hydrothermal flow conditions around a radioactive waste repository situated below the crest of a hill with a slope of one per mille. Permeability and porosity are constant. Vertical anisotropy. Release time: 360 years.

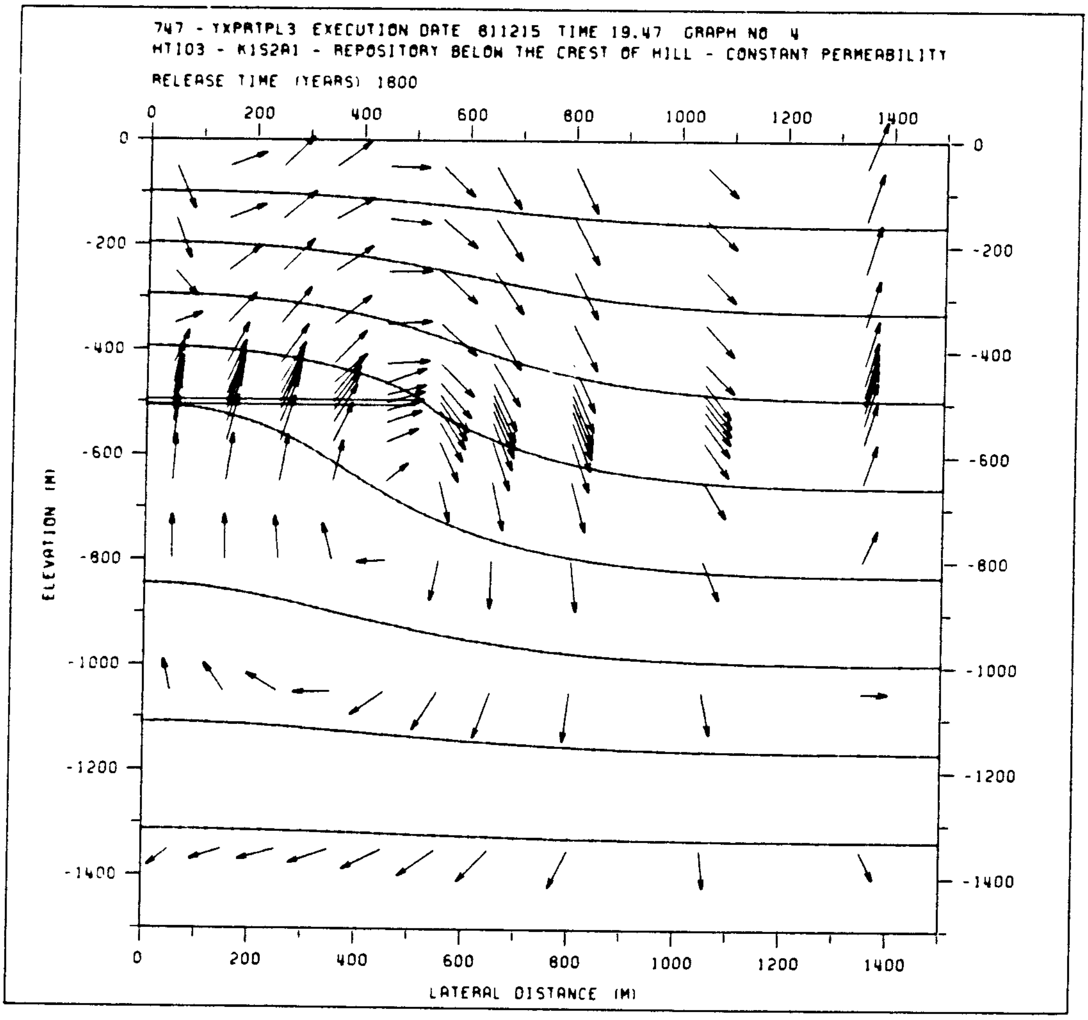


Figure 4.2.6 Groundwater fluxes and isotherms illustrating the hydrothermal flow conditions around a radioactive waste repository situated below the crest of a hill with a slope of one per mille. Permeability and porosity are constant. Vertical anisotropy. Release time: 1800 years.

4.2.2 Repository located below the crest of a hill with a slope of one per mille. Permeability and porosity are constant. Horizontal anisotropy.

Exit time: > 4100 years

> 9000 years without the influence of a repository

The results of the pathline trace are presented in tables 4.2.3 and 4.2.4.

Pathlines for the flow conditions with the influence of a repository are displayed in figure 4.2.7.

Pathlines for the natural flow conditions without the influence of a repository are displayed in figure 4.2.8.

Groundwater fluxes and isotherms are displayed in figures 4.2.9 - 4.2.12.

The most obvious effect of the horizontal anisotropy in this example is the considerably long travel times in comparison with those obtained in the previous example with vertical anisotropy. The effect of the heat released from the repository is to cause an uplift of the groundwater at the repository, with the exception of the area at the edges of the repository. A horizontal water divide is formed about 150 metres above the repository. Above this water divide the groundwater flow is essentially horizontal. Below the water divide a large convection cell is formed.

The flow velocities are relatively high during the initial period. When the effect of the heat begins to vanish, then the flow velocities become very low. Thus, after about 10000 years one can hardly observe any effect of the heat released from the repository.

The water particles traced from the repository are significantly affected by the convection currents. Thus, in the beginning the water particles move relatively fast, first upwards and then horizontally, towards the lateral boundaries of the flow domain. After some thousand years, the water particles are moving downwards at lower velocities. Then, the effect of the heat begin to vanish, and as a result the groundwater flow is again governed mainly by the topographical gradients. When the effect of the heat has vanished almost completely, one can see that the water particles have reached a region, where the flow velocities are extremely low. Subsequently, the travel times become very long for all water particles but one, namely the one starting from the centre of the repository. This water particle diverges from the other ones after about 3000 years. Then, it begins to move upwards instead of downwards, as the other ones do, and it reaches the ground surface after about 4000 years. As for the rest of the water particles, the travel times are computed to be over 60000 years.

For steady flow conditions the travel times become about 3 to 10 times longer in this case in comparison with the previous case, in which vertical anisotropy in the permeability was assumed. Thus, the travel time for a water particle starting at a distance of about 100 metres from the centre of the repository increased from about 5000 years to 60000 years, and the travel time for a water particle starting at the edge of the repository increased from about 3000 years to 9000 years.

Table 4.2.3 Coordinates of the starting respectively end points and the corresponding travel times in years of pathlines traced from a radioactive repository located below the crest of a hill with a slope of one per mille. Permeability and porosity are constant over the flow domain. Horizontal anisotropy.

| No | Starting point | | End point | | Travel time |
|---|---|---|---|---|---|
| 1 | 0 | -500 | 1480 | 0 | 4100 |
| 2 | 100 | -500 | 1500 | 0 | 69600 |
| 3 | 200 | -500 | - | - | >100000 |
| 4 | 300 | -500 | 1500 | 0 | 73100 |
| 5 | 400 | -500 | 1500 | 0 | 71600 |
| 6 | 500 | -500 | 1500 | 0 | 91400 |

Table 4.2.4 Coordinates of the starting respectively end points and the corresponding travel times in years of pathlines traced from a repository located below the crest of a hill with a slope of one per mille. Permeability and porosity are constant over the flow domain. Horizontal anisotropy. No heat is released from the repository.

| No | Starting point | | End point | | Travel time |
|---|---|---|---|---|---|
| 1 | 0 | -500 | - | - | >100000 |
| 2 | 100 | -500 | 1500 | 0 | 59200 |
| 3 | 200 | -500 | 1500 | 0 | 26500 |
| 4 | 300 | -500 | 1500 | 0 | 16600 |
| 5 | 400 | -500 | 1500 | 0 | 12000 |
| 6 | 500 | -500 | 1500 | 0 | 9270 |

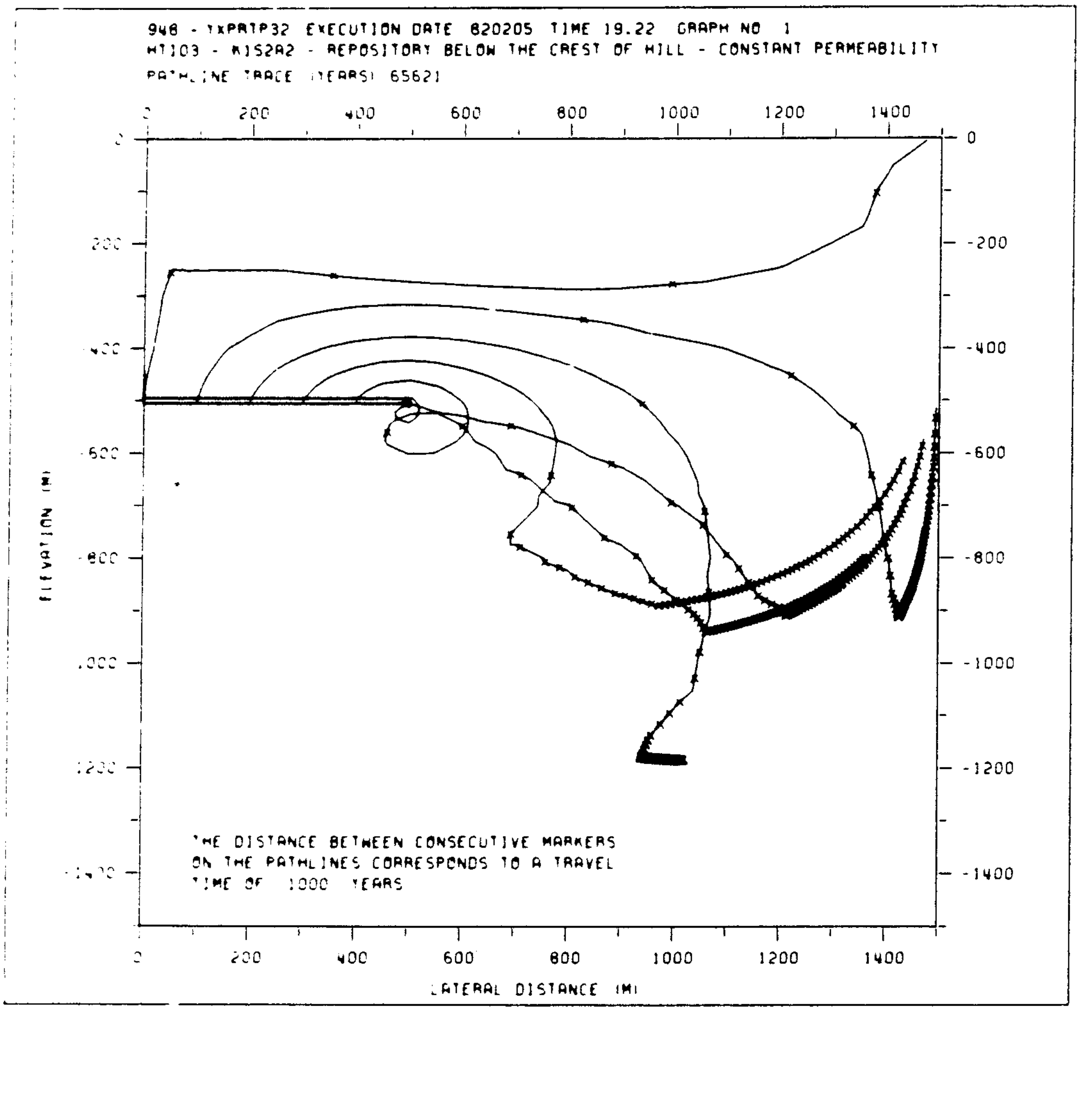


Figure 4.2.7 Pathlines for the flow conditions with the influence of a repository located below the crest of a hill with a slope of the hillsides of one per mille. Permeability and porosity are constant. Horizontal anisotropy.

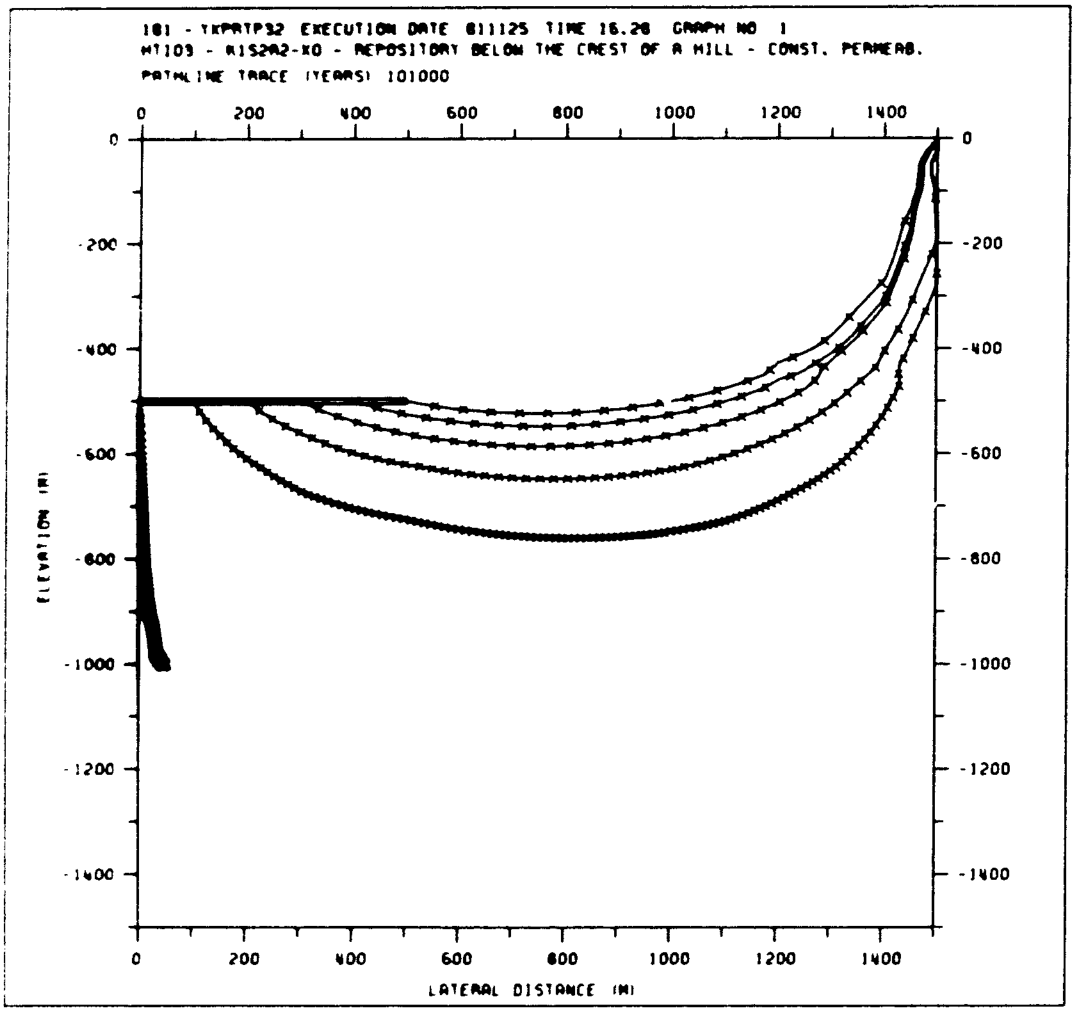


Figure 4.2.8 Pathlines for the natural flow conditions below the crest of a hill with a slope of one per mille. Permeability and porosity are constant. Horizontal anisotropy.

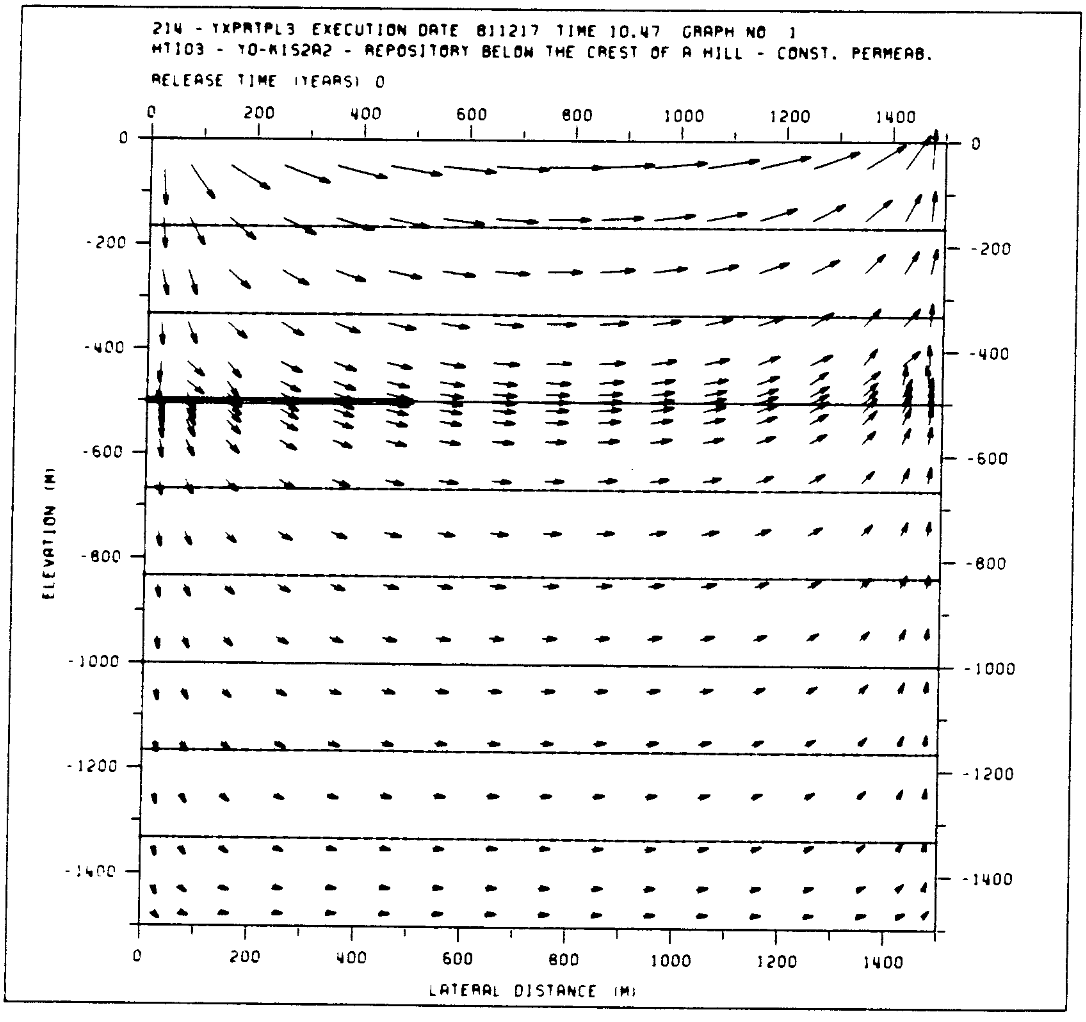


Figure 4.2.9 Groundwater fluxes and isotherms illustrating the hydrothermal flow conditions around a radioactive waste repository situated below the crest of a hill with a slope of one per mille. Permeability and porosity are constant. Horizontal anisotropy. Release time: 0 years.

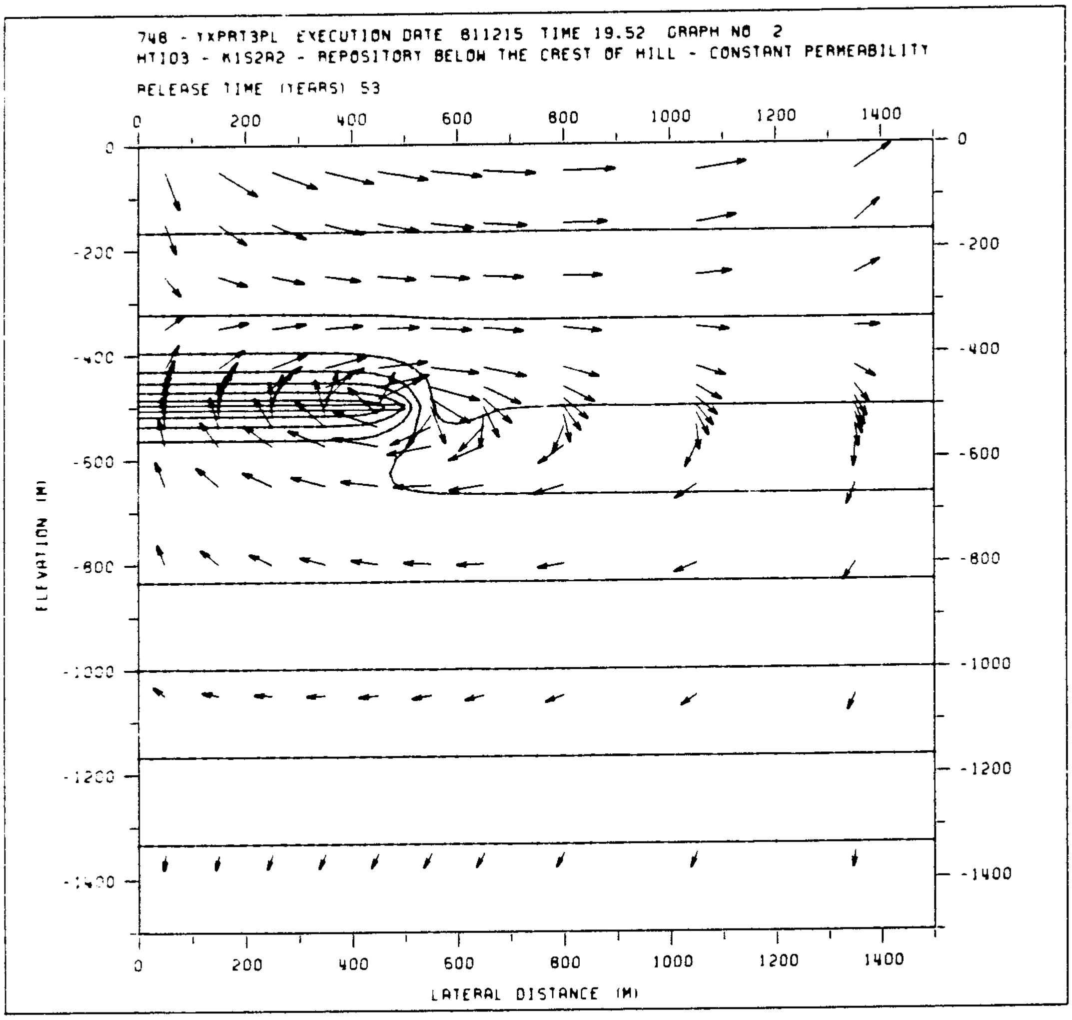


Figure 4.2.10 Groundwater fluxes and isotherms illustrating the hydrothermal flow conditions around a radioactive waste repository situated below the crest of a hill with a slope of one per mille. Permeability and porosity are constant. Horizontal anisotropy. Release time: 53 years.

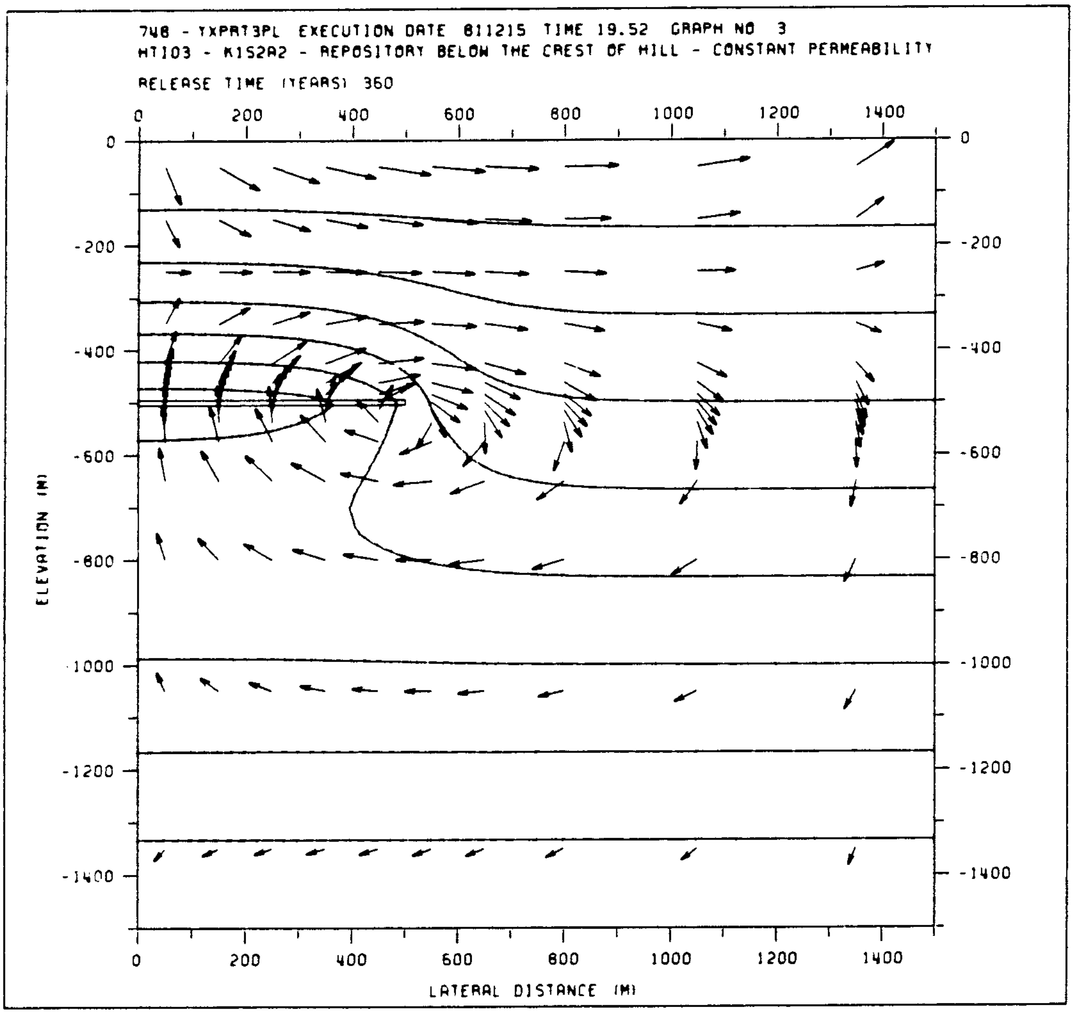


Figure 4.2.11 Groundwater fluxes and isotherms illustrating the hydrothermal flow conditions around a radioactive waste repository situated below the crest of a hill with a slope of one per mille. Permeability and porosity are constant. Horizontal anisotropy. Release time: 360 years.

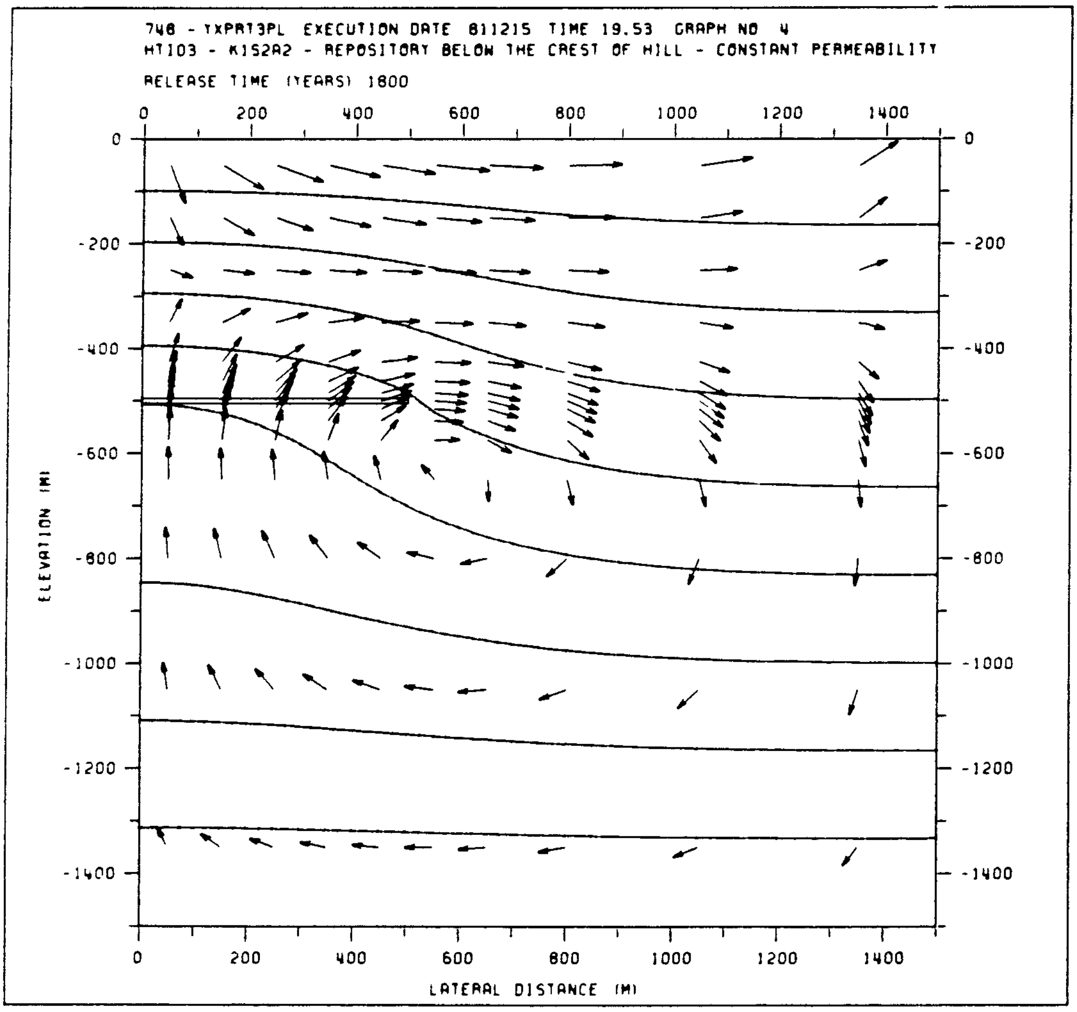


Figure 4.2.12 Groundwater fluxes and isotherms illustrating the hydrothermal flow conditions around a radioactive waste repository situated below the crest of a hill with a slope of one per mille. Permeability and porosity are constant. Horizontal anisotropy. Release time: 1800 years.

4.2.3 Repository located below the crest of a hill with a slope of one per mille. Permeability and porosity decrease exponentially with depth. Vertical anisotropy.

Exit time: > 5800 years

> 4500 years without the influence of a repository

The results of the pathline trace are presented in tables 4.2.5 and 4.2.6.

Pathlines for the flow conditions with the influence of a repository are presented in figure 4.2.13.

Pathlines for the natural flow conditions without the influence of a repository are displayed in figure 4.2.14.

Groundwater fluxes and isotherms are displayed in figures 4.2.15 - 4.2.18.

Convection currents are formed at the edges of the repository, but the effect on the travel times seems to be fairly moderate. The effect of the heat released from the repository is essentially to prolong the travel times. Initially, the groundwater flow is horizontal in most part of the flow domain. The consequence of the convection currents, formed around the edges of the repository, is that the flow paths from the repository are getting closer to the ground surface. Despite this fact, the travel times become longer for all of the traced water particles. The water particle starting from the centre of the repository should in principle follow the flow domain boundary, but the decrease in permeability with depth, together with the coarseness of the elements along the boundary, will restrain the downward movement of this water particle.

Table 4.2.5 Coordinates of the starting respectively end points and the corresponding travel times in years of pathlines traced from a radioactive repository located below the crest of a hill with a slope of one per mille. Permeability and porosity decrease exponentially with depth. Vertical anisotropy.

| No | Starting point | | End point | | Travel time |
|---|---|---|---|---|---|
| 1 | 0 | -500 | 1500 | 0 | 9274 |
| 2 | 100 | -500 | 1500 | 0 | 6647 |
| 3 | 200 | -500 | 1500 | 0 | 6229 |
| 4 | 300 | -500 | 1500 | 0 | 5896 |
| 5 | 400 | -500 | 1500 | 0 | 5850 |
| 6 | 500 | -500 | 1500 | 0 | 6267 |

Table 4.2.6 Coordinates of the starting respectively end points and the corresponding travel times in years of pathlines traced from a repository located below the crest of a hill with a slope of one per mille. Permeability and porosity decrease exponentially with depth. Vertical anisotropy. No heat is released from the repository.

| No | Starting point | | End point | | Travel time |
|---|---|---|---|---|---|
| 1 | 0 | -500 | 1500 | 0 | 8640 |
| 2 | 100 | -500 | 1500 | 0 | 5440 |
| 3 | 200 | -500 | 1500 | 0 | 5220 |
| 4 | 300 | -500 | 1500 | 0 | 5080 |
| 5 | 400 | -500 | 1500 | 0 | 4740 |
| 6 | 500 | -500 | 1500 | 0 | 4500 |

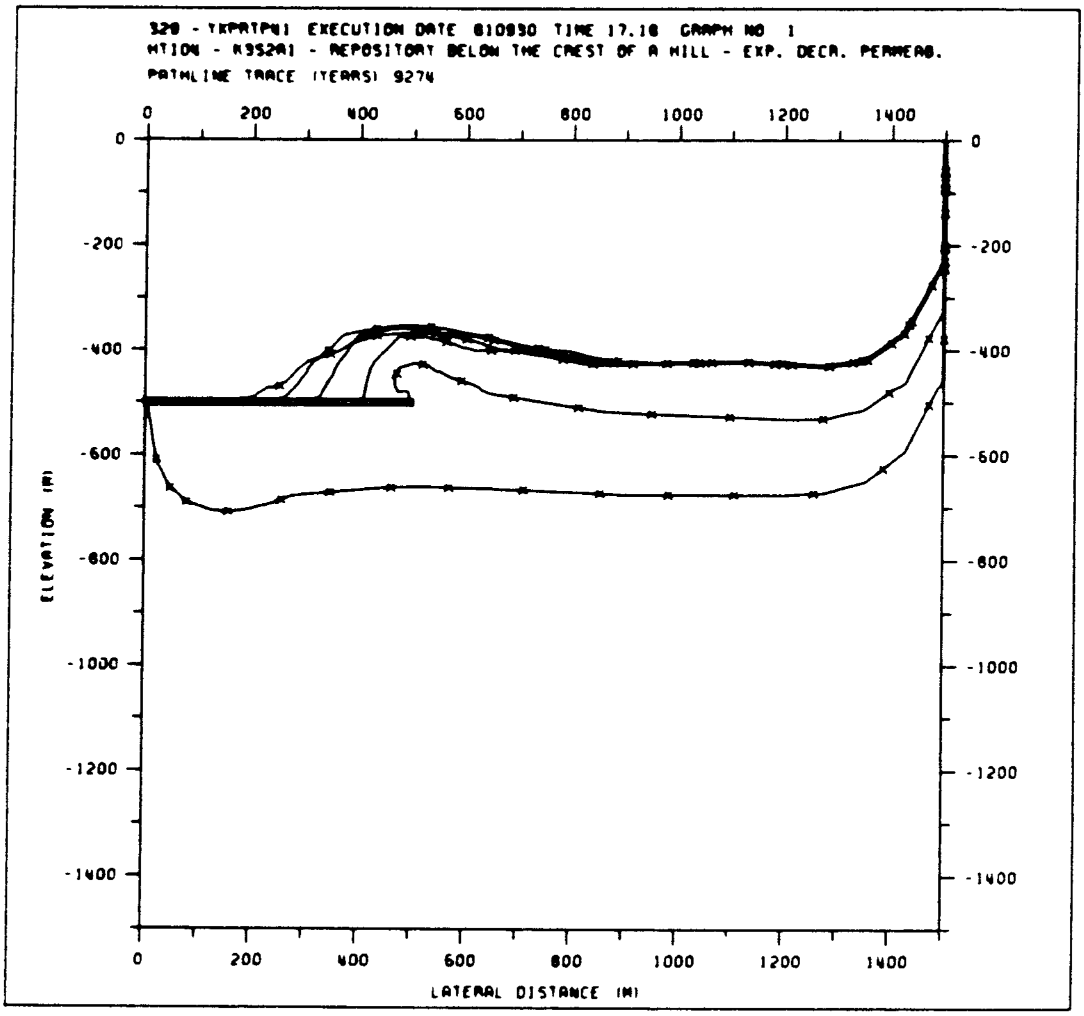


Figure 4.2.13 Pathlines for the flow conditions with the influence of a repository located below the crest of a hill with a slope of one per mille. Permeability and porosity decrease exponentially with depth. Vertical anisotropy.

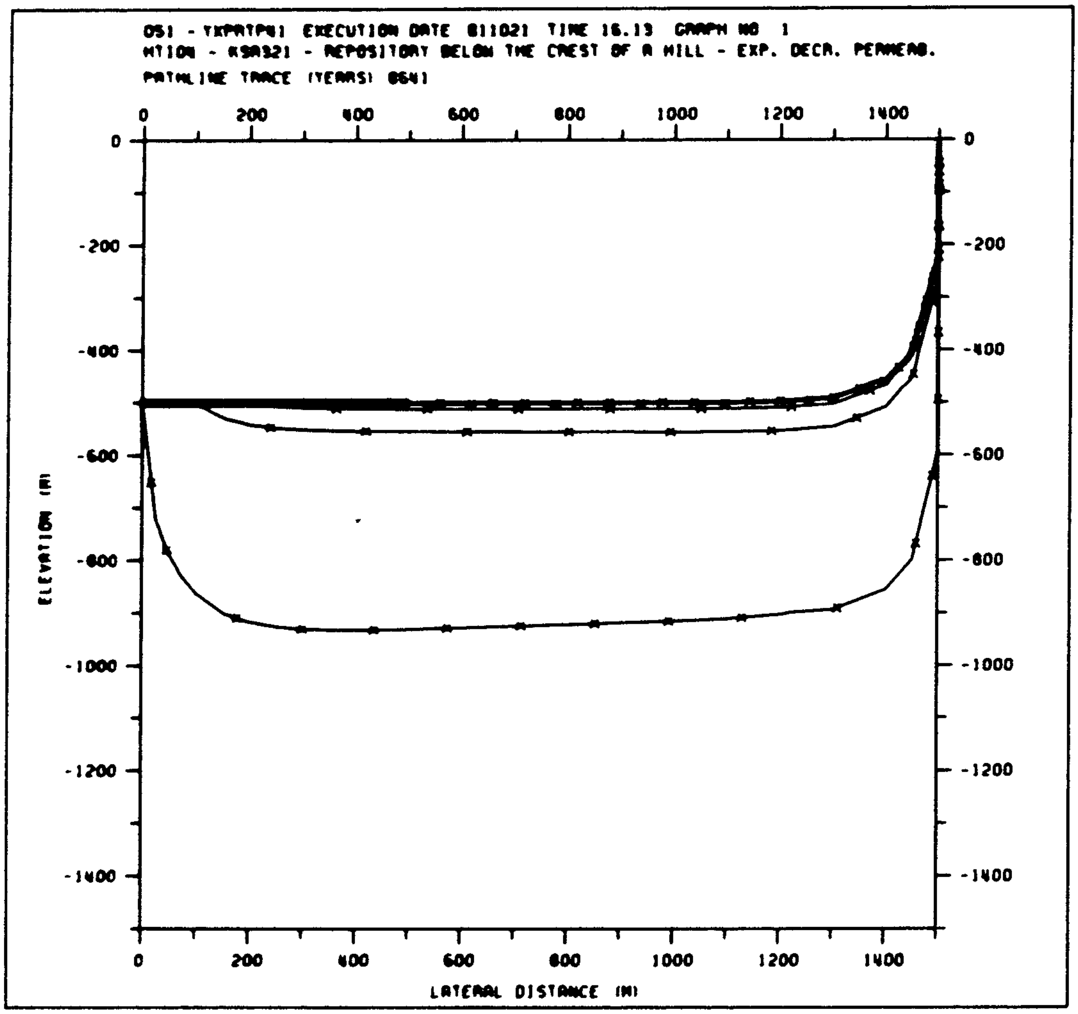


Figure 4.2.14 Pathlines for the natural flow conditions below the crest of a hill with a slope of one per mille. Vertical anisotropy. Permeability and porosity decrease exponentially with depth.

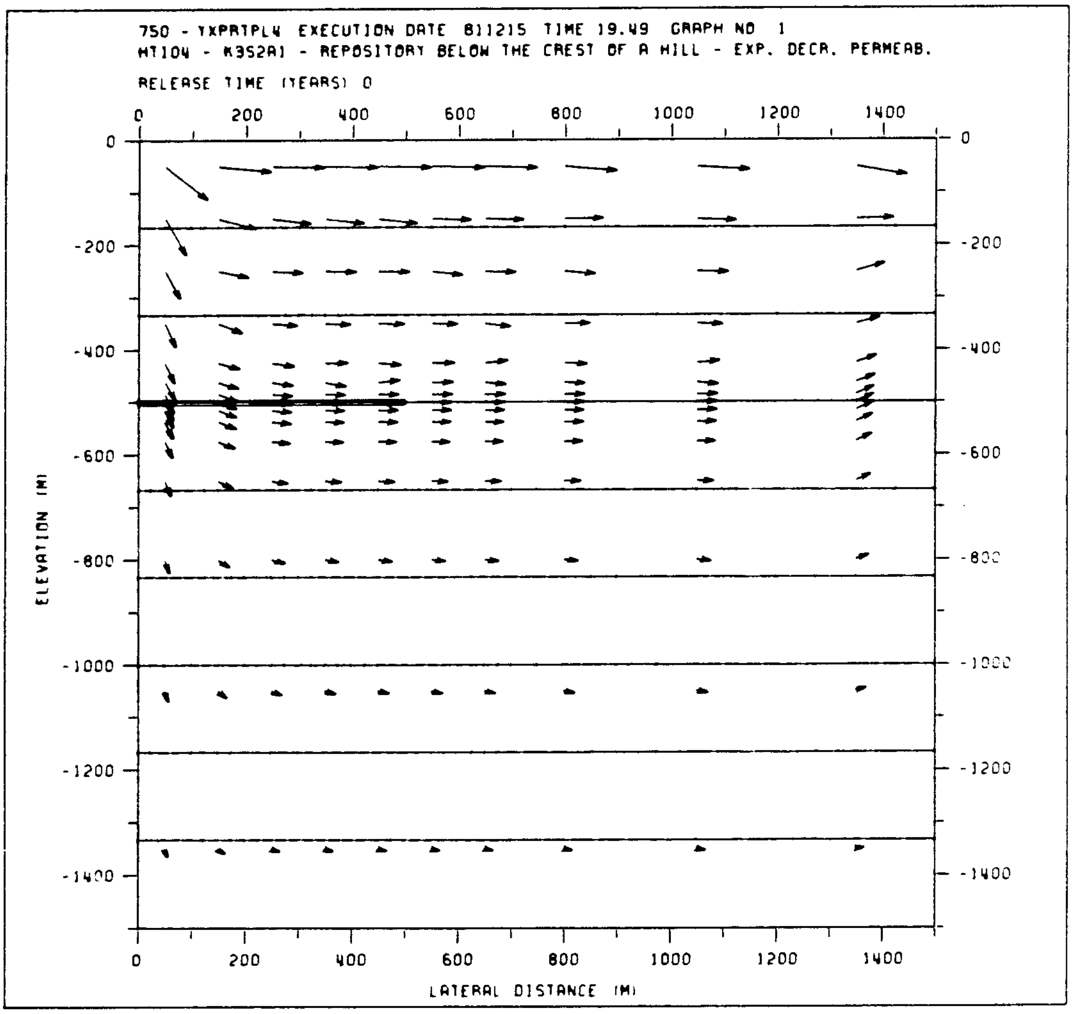


Figure 4.2.15 Groundwater fluxes and isotherms illustrating the hydrothermal flow conditions around a radioactive waste repository situated below the crest of a hill with a slope of one per mille. Permeability and porosity decrease exponentially with depth. Vertical anisotropy. Release time: 0 years.

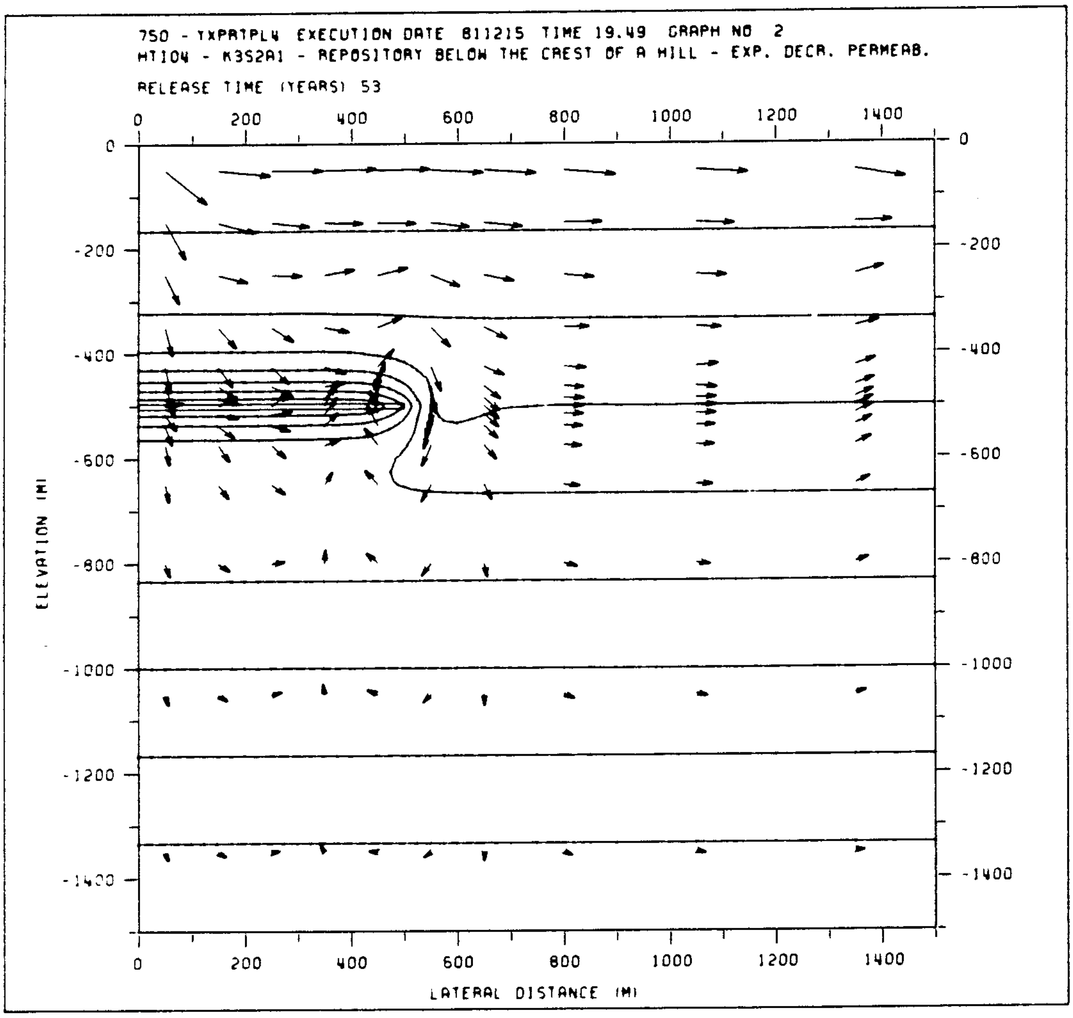


Figure 4.2.16 Groundwater fluxes and isotherms illustrating the hydrothermal flow conditions around a radioactive waste repository situated below the crest of a hill with a slope of one per mille. Permeability and porosity decrease exponentially with depth. Vertical anisotropy. Release time: 53 years.

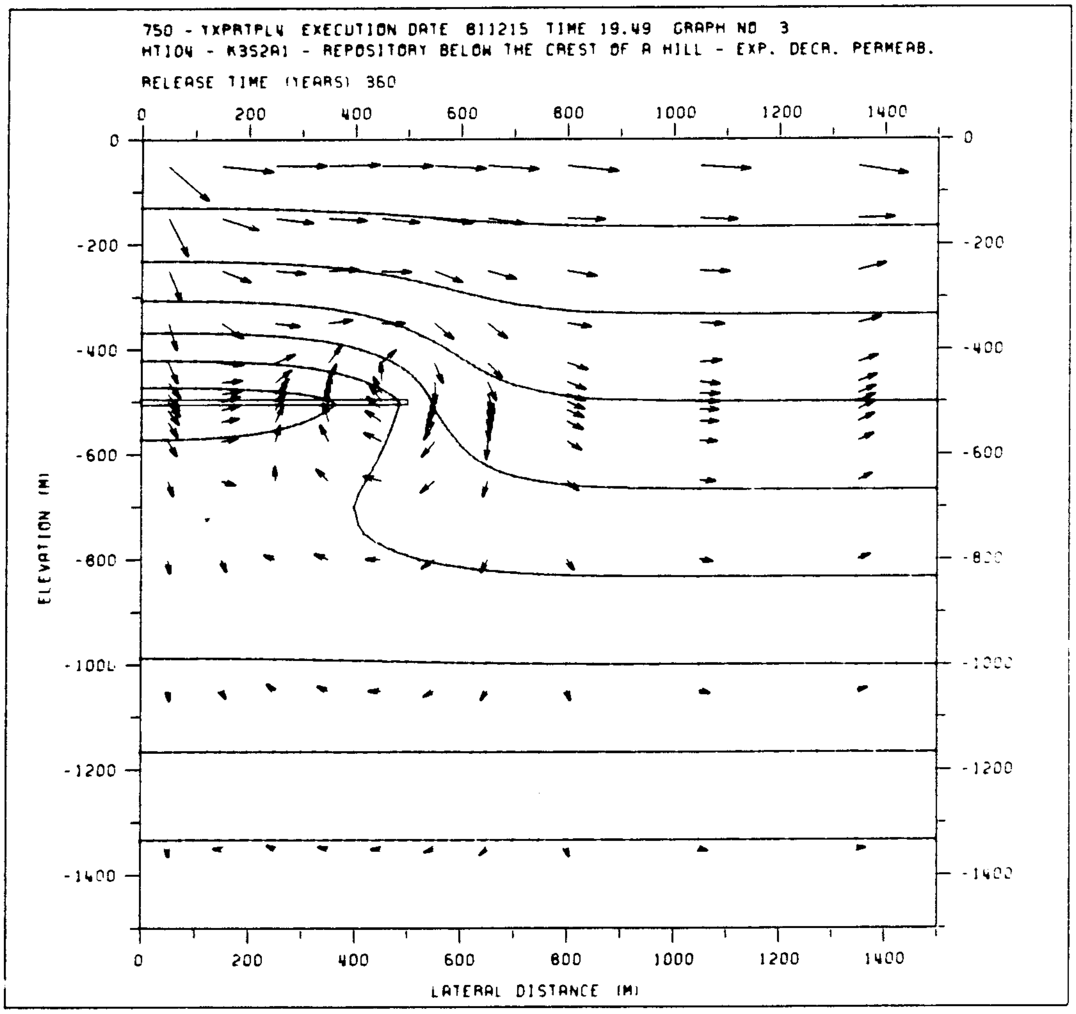


Figure 4.2.17 Groundwater fluxes and isotherms illustrating the hydrothermal flow conditions around a radioactive waste repository situated below the crest of a hill with a slope of one per mille. Permeability and porosity decrease exponentially with depth. Vertical anisotropy. Release time: 360 years.

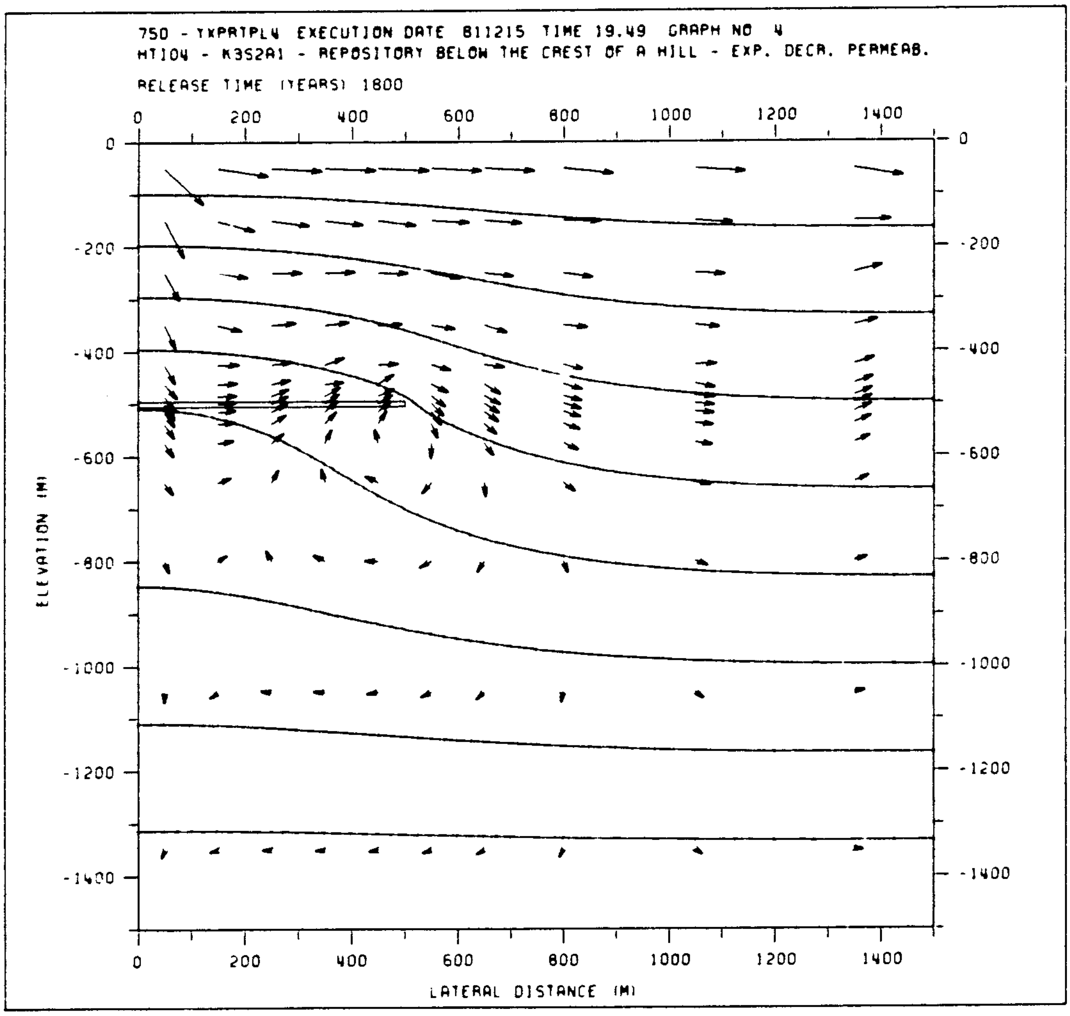


Figure 4.2.18 Groundwater fluxes and isotherms illustrating the hydrothermal flow conditions around a radioactive waste repository situated below the crest of a hill with a slope of one per mille. Permeability and porosity decrease exponentially with depth. Vertical anisotropy. Release time: 1800 years.

### 4.2.4 Repository located below the crest of a hill with a slope of one per mille. Permeability and porosity decrease exponentially with depth. Horizontal anisotropy.

Exit time: > 4100 years

> 3200 years without the influence of a repository

The results of the pathline trace are presented in tables 4.2.7 and 4.2.8.

Pathlines for the flow conditions with the influence of a repository are presented in figure 4.2.19.

Pathlines for the natural flow conditions without the influence of a repository are displayed in figure 4.2.20.

Groundwater fluxes and isotherms are displayed in figures 4.2.21 - 4.2.24.

As in the previous case with vertical anisotropy, the groundwater flow is largely horizontal in the flow domain. Comparing the present results with the ones obtained from vertical anisotropy, it turns out that horizontal anisotropy gives shorter travel times for the water particles starting at 100 respectively 200 metres from the centre of the repository, but longer travel times for the rest of the traced water particles. Similarly, comparing the travel times for steady flow, it appears that the travel times become shorter for all but two of the water particles traced from the repository, namely the ones starting at the centre of the repository.

Table 4.2.7 Coordinates of the starting respectively end points and the corresponding travel times in years of pathlines traced from a radioactive repository located below the crest of a hill with a slope of one per mille. Permeability and porosity decrease exponentially with depth. Horizontal anisotropy.

| No | Starting point | | End point | | Travel time |
|---|---|---|---|---|---|
| 1 | 0 | -500 | 1500 | 0 | 7810 |
| 2 | 100 | -500 | 1500 | 0 | 4110 |
| 3 | 200 | -500 | 1500 | 0 | 4550 |
| 4 | 300 | -500 | 1500 | 0 | 7030 |
| 5 | 400 | -500 | 1500 | 0 | 6040 |
| 6 | 500 | -500 | 1500 | 0 | 6960 |

Table 4.2.8 Coordinates of the starting respectively end points and the corresponding travel times in years of pathlines traced from a repository located below the crest of a hill with a slope of one per mille. Permeability and porosity decrease exponentially with depth. Horizontal anisotropy. No heat is released from the repository.

| No | Starting point | | End point | | Travel time |
|---|---|---|---|---|---|
| 1 | 0 | -500 | 1500 | 0 | 22570 |
| 2 | 100 | -500 | 1500 | 0 | 6060 |
| 3 | 200 | -500 | 1500 | 0 | 4790 |
| 4 | 300 | -500 | 1500 | 0 | 4100 |
| 5 | 400 | -500 | 1500 | 0 | 3650 |
| 6 | 500 | -500 | 1500 | 0 | 3250 |

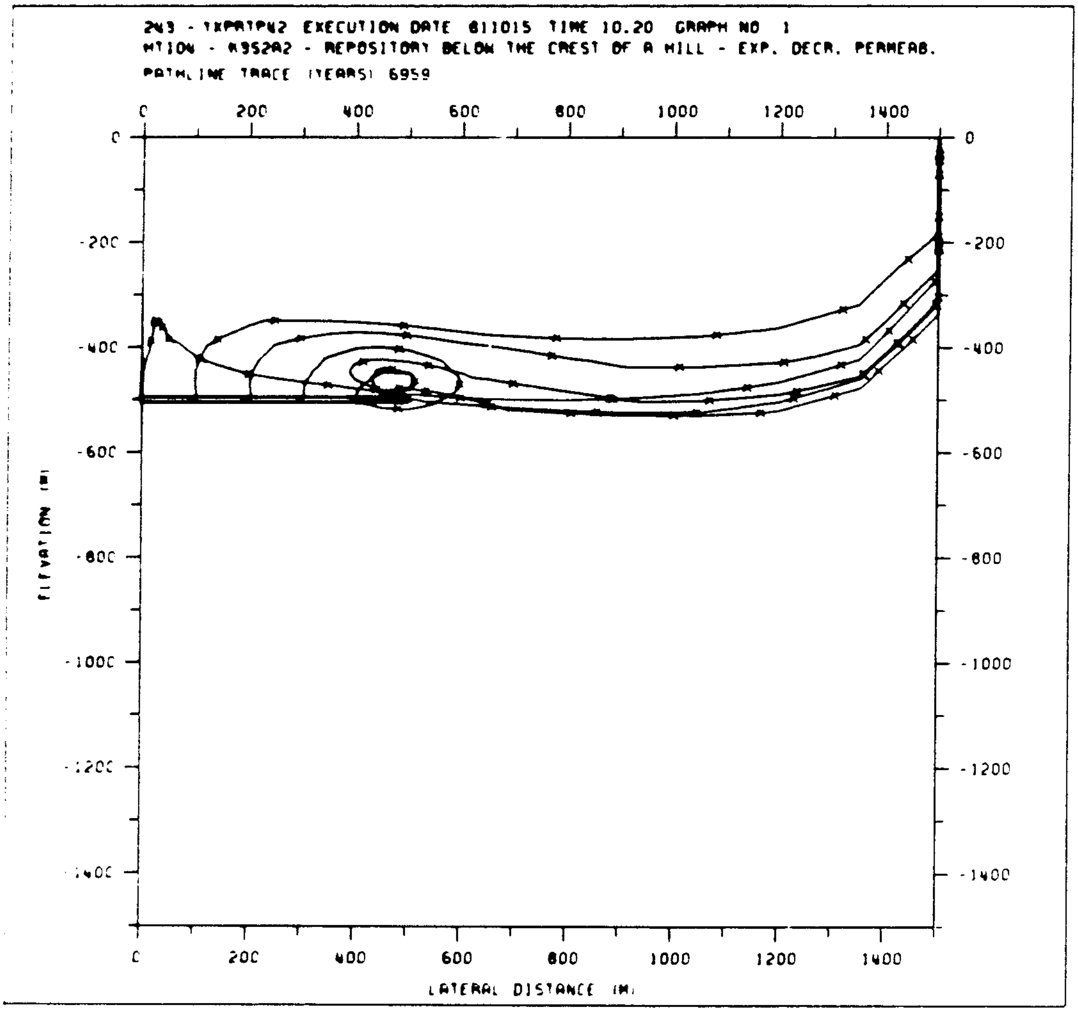


Figure 4.2.19 Pathlines for the flow conditions with the influence of a repository located below the crest of a hill with a slope of one per mille. Permeability and porosity decrease exponentially with depth. Horizontal anisotropy.

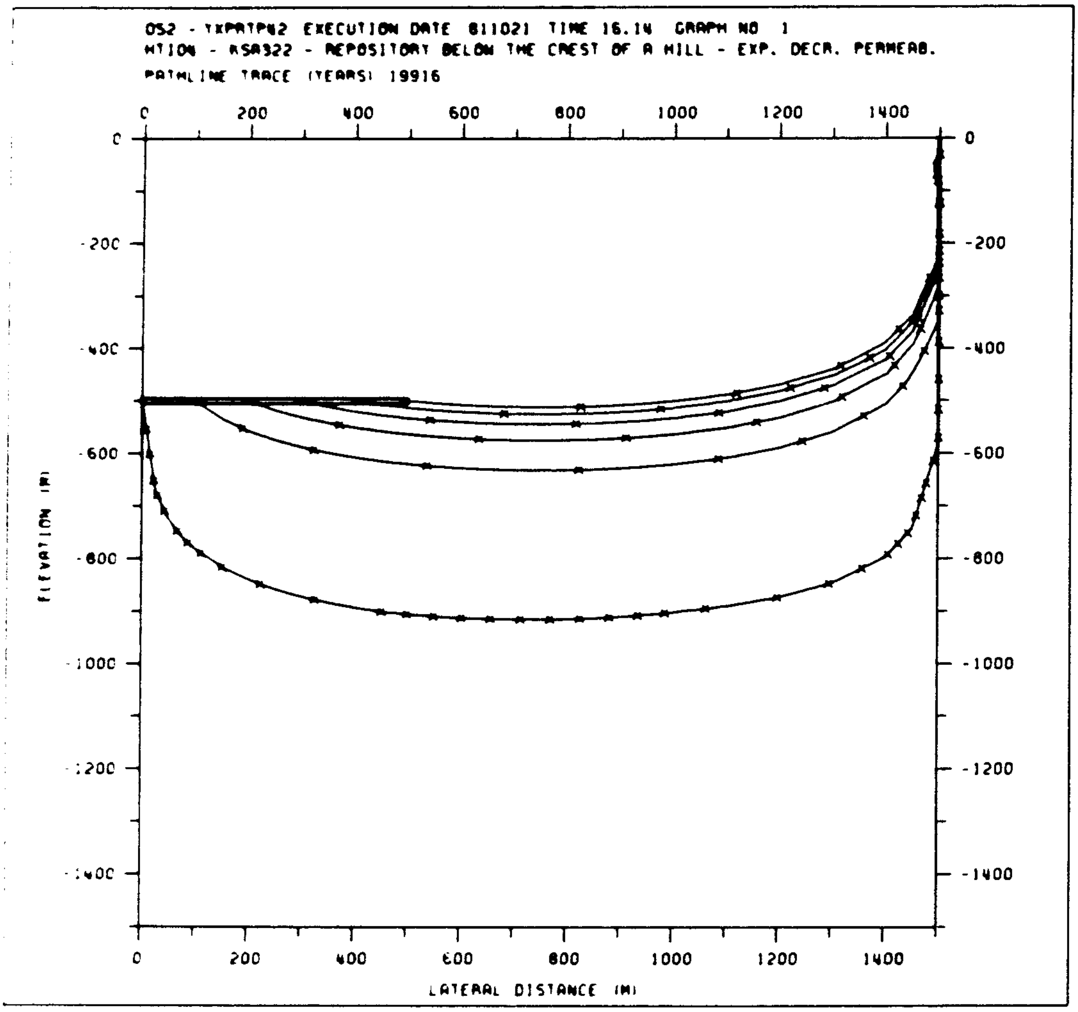


Figure 4.2.20 Pathlines for the natural flow conditions below the crest of a hill with a slope of one per mille. Permeability and porosity decrease exponentially with depth. Horizontal anisotropy.

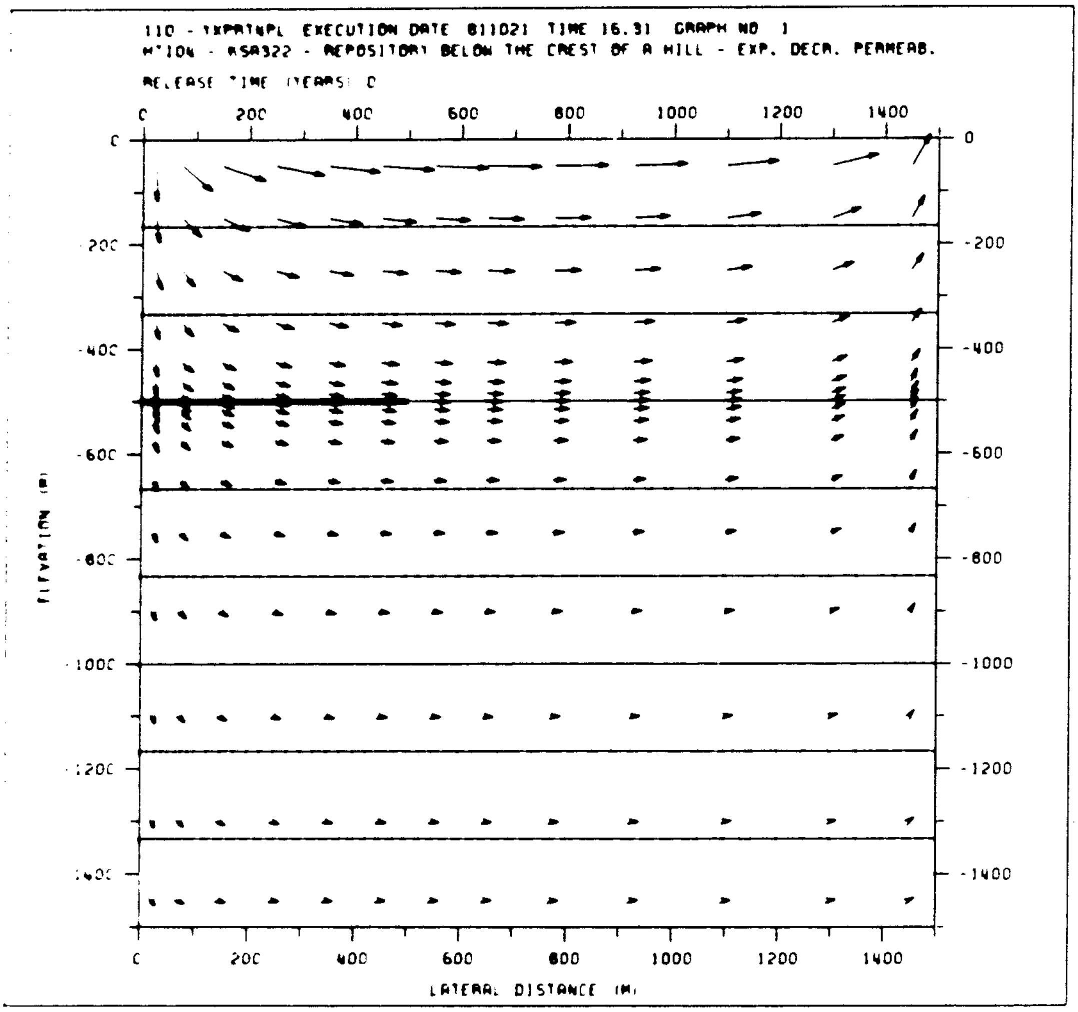


Figure 4.2.21 Groundwater fluxes and isotherms illustrating the hydrothermal flow conditions around a radioactive waste repository situated below the crest of a hill with a slope of one per mille. Permeability and porosity decrease exponentially with depth. Horizontal anisotropy. Release time: 0 years.

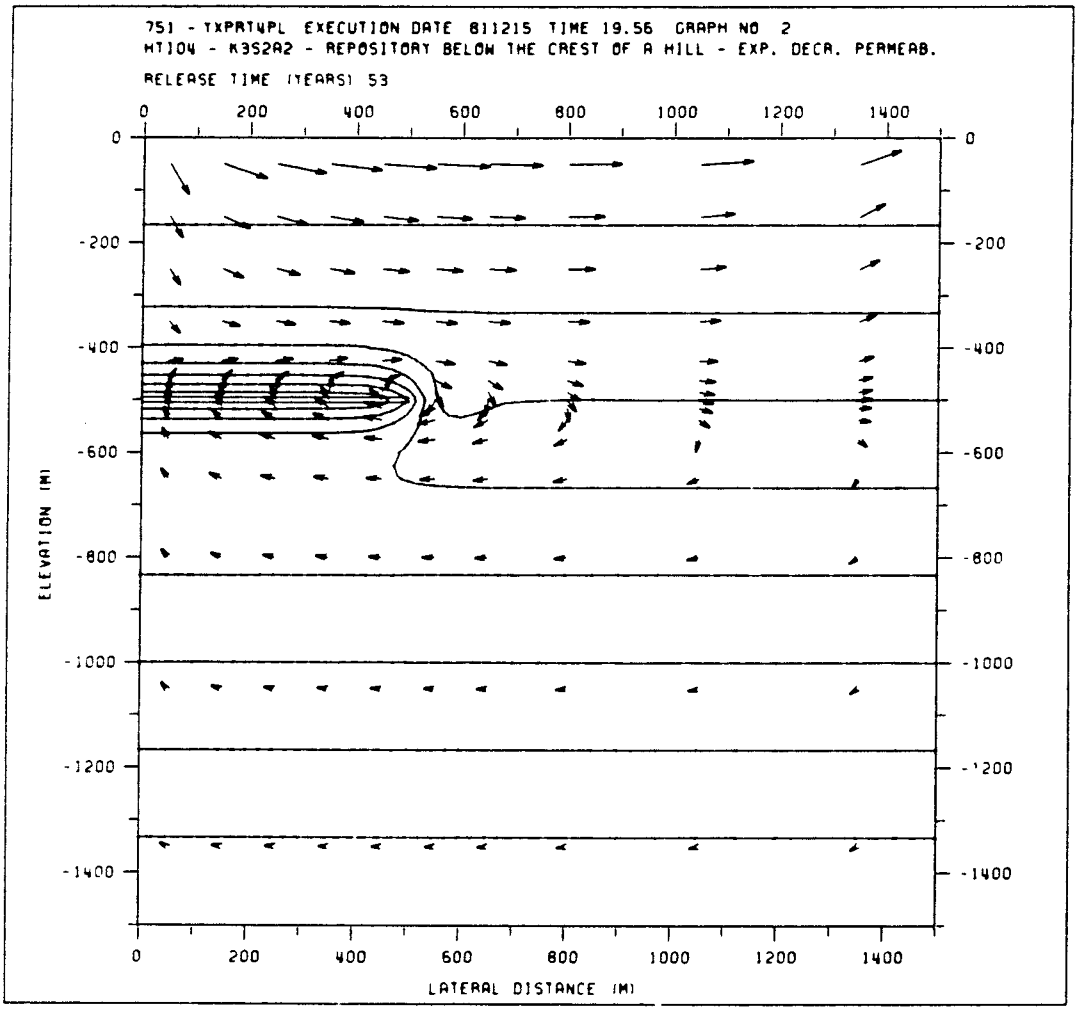


Figure 4.2.22 Groundwater fluxes and isotherms illustrating the hydrothermal flow conditions around a radioactive waste repository situated below the crest of a hill with a slope of one per mille. Permeability and porosity decrease exponentially with depth. Horizontal anisotropy. Release time: 53 years.

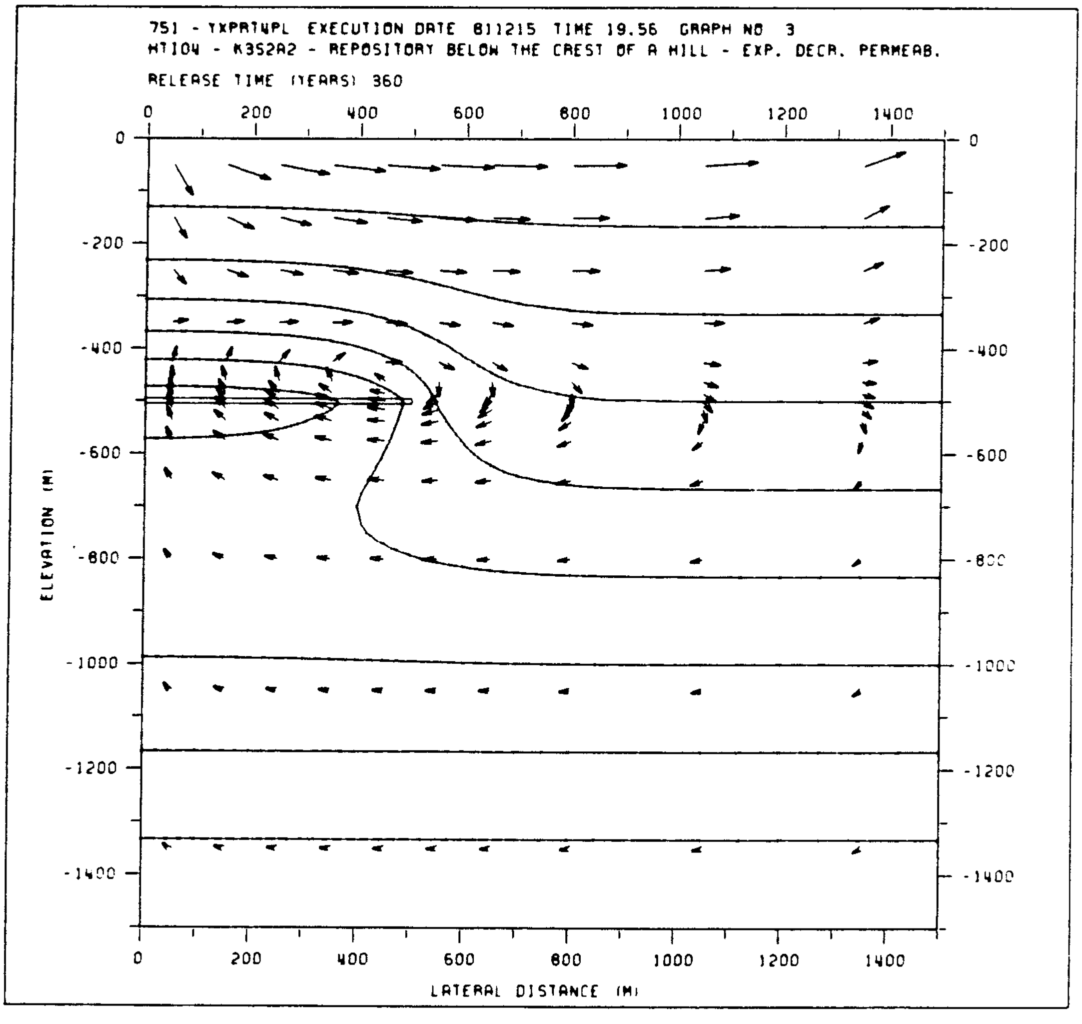


Figure 4.2.23 Groundwater fluxes and isotherms illustrating the hydrothermal flow conditions around a radioactive waste repository situated below the crest of a hill with a slope of one per mille. Permeability and porosity decrease exponentially with depth. Horizontal anisotropy. Release time: 360 years.

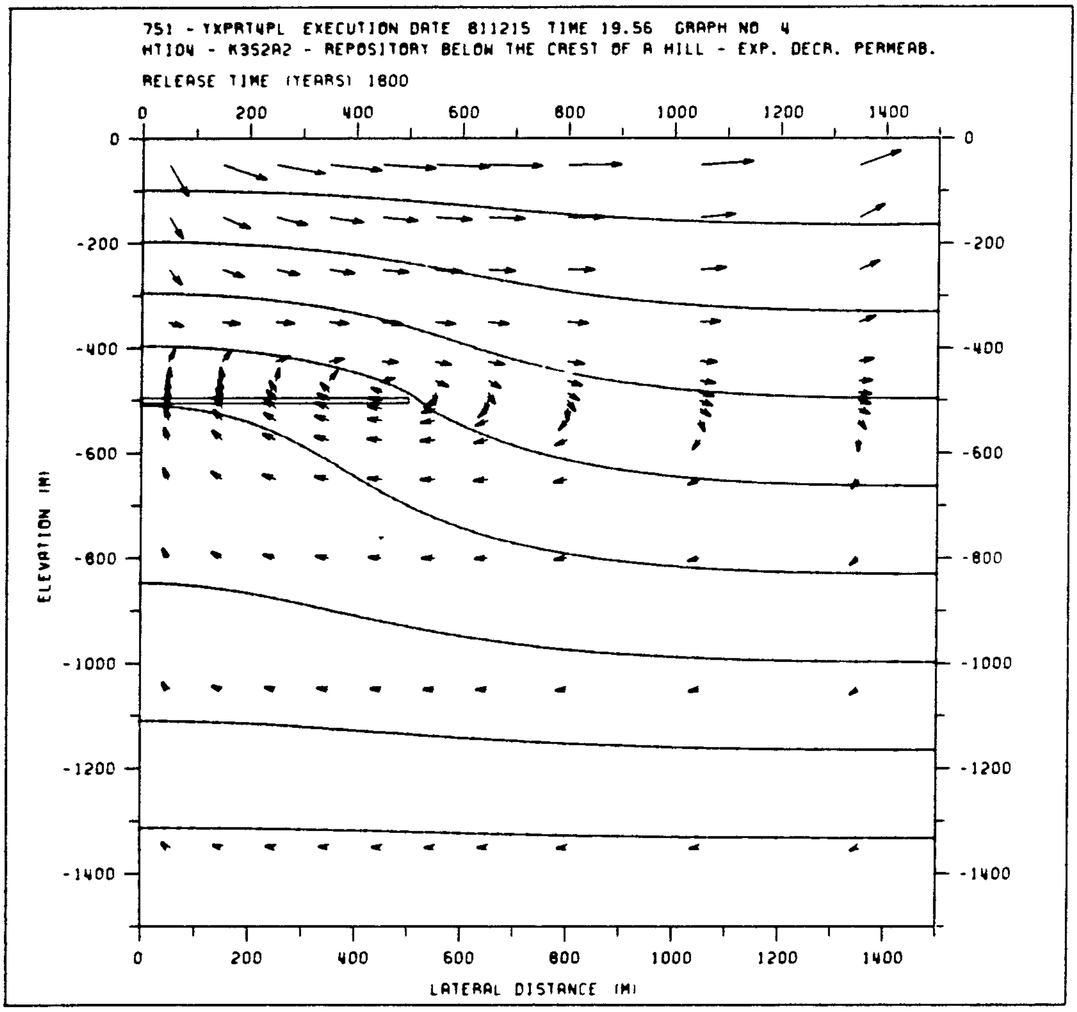


Figure 4.2.24 Groundwater fluxes and isotherms illustrating the hydrothermal flow conditions around a radioactive waste repository situated below the crest of a hill with a slope of one per mille. Permeability and porosity decrease exponentially with depth. Horizontal anisotropy. Release time: 1800 years.

## 5. REFERENCES

1 Thunvik, R. and Braester, C., 1980, HYDROTHERMAL CONDITIONS AROUND A RADIOACTIVE WASTE REPOSITORY, Part 1 - A Mathematical Model for the Flow of Groundwater and Heat in Fractured Rocks, Part 2 - Numerical Solutions, SKBF-KBS-TR-80-19.

FÖRTECKNING ÖVER KBS TEKNISKA RAPPORTER

1977-78

TR 121 KBS Technical Reports 1 - 120.
Summaries. Stockholm, May 1979.

1979

TR 79-28 The KBS Annual Report 1979.
KBS Technical Reports 79-01--79-27.
Summaries. Stockholm, March 1980.

1980

TR 80-26 The KBS Annual Report 1980.
KBS Technical Reports 80-01--80-25.
Summaries. Stockholm, March 1981.

1981

TR 81-17 The KBS Annual Report 1981.
KBS Technical Reports 81-01--81-16
Summaries. Stockholm, April 1982.

1982

TR 82-01 Hydrothermal conditions around a radioactive waste repository
Part 3 - Numerical solutions for anisotropy
Roger Thunvik
Royal Institute of Technology, Stockholm, Sweden
Carol Braester
Institute of Technology, Haifa, Israel
December 1981